M.Sc. Thesis

ROCK BURSTS ANALYSIS OF PARALLEL TUNNELS USING NUMERICAL MODELLING

Author

Sohail Manzoor
2013-MS-Min-01

Supervisor

Dr. Muhammad Zaka Emad
Assistant Professor

DEPARTMENT OF MINING ENGINEERING
FACULTY OF EARTH SCIENCES and ENGINEERING
UNIVERSITY OF ENGINEERING AND TECHNOLOGY, LAHORE

June 2017

ROCK BURSTS ANALYSIS OF PARALLEL TUNNELS USING NUMERICAL MODELLING

Author

Sohail Manzoor

2013-MS-Min-01

A thesis submitted in partial fulfillment of the requirement for the degree of

M.Sc. Mining Engineering

Thesis Supervisor:

Dr. Muhammad Zaka Emad

Assistant Professor

Department of Mining Engineering

Signature: _____

(Dr. Muhammad Zaka Emad)

Thesis Supervisor/Internal Examiner

Signature: _____

(Prof. (R) Dr. Syed M. Tariq)

External Examiner

Signature: _____

(Dr. Zulfiqar Ali)

Department Chairman

Signature: _____

(Prof. Dr. Nadeem Feroze)

Faculty Dean

DEPARTMENT OF MINING ENGINEERING
FACULTY OF EARTH SCIENCES and ENGINEERING
UNIVERSITY OF ENGINEERING AND TECHNOLOGY, LAHORE

June 2017

ABSTRACT

One of the essential components of the underground excavation design process, which directly influences the performance and stability of underground constructions, is knowledge of the in-situ and mining-induced stress. Knowing the magnitudes and directions of these stresses can help determine suitable shapes and orientations for tunnels (drifts) and stopes. In addition, knowing the stress regime in the rock mass can be used to predict the type of rock failure that may occur in the future and identify potential rockbursting zones.

In this research, the main objective is to develop an engineering methodology to estimate the mining-induced stress regimes in the host rock and orebody using the finite element analysis method. A potential hydro-electric project site is used to illustrate the estimation procedure and to implement the proposed methodology.

To reach the objectives of this research, 2-dimensional finite element models of the project site were developed. These finite element analysis models were used to determine the mining-induced stress regimes at the potential hydro-electric project site. The results of FE analysis were used in combination with tangential stress criterion for rock burst assessment in parallel tunnels.

The main contributions of this study include developing and implementing an engineering methodology for estimating mining-induced stresses, providing a better understanding of the stress distribution regime around a tunnel and investigating the role of overburden thickness and excavation sequence on mining-induced stress fields.

Keywords: Stress, Rock burst, Finite Element numerical modelling, Rock mass classification

UNDERTAKING

I certify that research work titled "*ROCK BURSTS ANALYSIS OF PARALLEL TUNNELS USING NUMERICAL MODELLING*" is my own work. The work has not been presented elsewhere for assessment. Where material has been used from other sources it has been properly acknowledged / referred.

Sohail Manzoor

2013-MS-Min-01

ACKNOWLEDGEMENTS

I am most thankful to my Allah, who enabled me to accomplish this milestone, and my parents for their lifetime unconditional love, support and encouragements. I owe my love and gratitude to my lovely wife, who believed in me and stood by my side to pursue my research work. I thank her for the patience and continuous encouragements and inspirations during this research.

I would like to thank my supervisor Dr. Muhammad Zaka Emad for his continued encouragements and guidance during this research. Without his leadership, support, time and energy he committed to help me, I would not be able to accomplish this research.

I would like to express my gratitude and appreciation to Dr. Zulfiqar Ali, Chairman Mining Engineering Department, for his continuous support and for providing me the facility to use Mine Design and Simulation Lab on weekends.

I would like to specially thank Dr. Muhammad Zubair Abu Bakar, Chairman Geological Engineering Department, for helping me in acquiring field data and guiding me through his valuable suggestions.

Sohail Manzoor, June 2017

Contents

List of Figures

List of Tables

Chapter 1 INTRODUCTION

1.1 General

Rock burst is a geotechnical hazard experienced by underground excavations. It occurs when there is high overburden in tandem with high in-situ stresses (Khanlari and Ghaderi-Meybodi, 2011). At a seminar on 10 November 1983 E. T. Brown said, "It is difficult to reach an agreement on the definition of rock burst" (Brown, 1988). This is because many researchers had different understanding of rock burst mechanism depending upon the case studies they observed. Generally, when a deep underground tunnel or chamber is excavated in strong and brittle rock, the change in stresses may result in dynamic damage to adjacent rock that is commonly known as rock burst. It can be grouped with seismic event and it is the damage to excavation done in rapid and violent manner (Kaiser, et al., 1996). Rock bursts are dangerous to the safety of workers and equipment as well as it affects the shape and size of the structure (Jiang, et al., 2010).

British coal mine at Stafford in 1938, first time reported the rock burst (Jiang, et al., 2010). After that, there have been several reports of rock bursts all around the world. Over the past few years, the importance of this hazard has led to various changes in infrastructures such as tunneling and mining. It has been drawing attention since it was experienced for the first time. The major contributing factors for initiation of rock bursts include structural geology and mining activities as discussed in Table 1.1. Rock bursts in mines and tunnels are frequently analyzed by the numerical modeling during long term and short range planning (Sharan, 2007). By comparing finite element results with analytical solutions for deep circular openings in rock mass subject to hydrostatic in situ stress, effectiveness and efficiency of the proposed numerical technique can be presented.

Due to current energy crisis, the Government of Pakistan has started many projects for power generation. Many hydro-electric power projects are underway in northern areas of the country due to economical source of power generation. But, some of the projects are experiencing rock bursts that are damaging the excavation process and causing safety issues. To provide the preventive measures and predict the major source of rock bursts, there is a need to study and evaluate the excavation process and tunnel design parameters. In this research, parallel headrace tunnels of a hydro-electric project site are modelled using finite element software that is RS^2 (Rocscience Inc.) to determine the causes of rock bursts. The rock mass rating

(RMR) and rock quality index (Q) are also determined for the tunneling site. Based on the findings, new strategy for tunnel construction is devised and recommendations are made.

1.2 Background

With the increase in mining depth, serious stability and safety issue arise most common of which is occurrence of seismic activity. The in-situ stress increases many folds at greater depths. Mining activity also induce change in stress magnitude and direction. The additional stresses may concentrate in some regions. This concentrated stress becomes destructive and causes energy to build up leading to a potential seismic activity. A seismic event is transient dynamic stress wave due to rock fracturing (Kabwe and Wang, 2015). Here it is necessary to distinguish between a rock burst and a seismic event. A seismic event may not essentially be a source of damage in excavations, whereas a rock burst will cause damage, with erratic damage severity as shown in Figure 1.1. This means that all rock bursts are seismic events but all seismic events are not rock bursts.

Figure 1.1: Rock burst damage in a hydropower tunnel (After Yu, et al., 2015)

The source of rock burst can either be located right at the location of damage zone or it can be located some distance away from the damage site. Therefore, rock bursts can be classified into self-initiated and remotely triggered rock bursts (Woldemedhin and Mwagalanyi, 2011).

There are two types of driving sources of rock bursts: except for the strain energy that accumulates in the local rock mass, the external energy transfer is the driving source for a small proportion of rock bursts; that is, $E_{\text{drive}} = E_{\text{local}} + E_{\text{transfer}}$. A stronger rock burst is initiated by the combination of the above types, as a stronger strong rock burst can initiate a

new rock burst in nearby rock (Kabwe and Wang, 2015). The same phenomenon is observed by Gu et al. (2014) in a laboratory rock burst study.

There are various parameters that effect rock burst damage and its severity. Table 1.1 summarizes the main factors contributing to rock burst damage. The Table also groups them into four categories, that is seismic event, geology, geotechnical, and mining. Factors in the first two groups (seismic event and geology) determine the intensity of dynamic load at the damage locations, and the factors in the last two groups (geotechnical and mining) determine site response due to seismic impulses. Rock burst damage is therefore governed by a combination of these factors.

Table 1.1: Main factors influencing rock burst damage (After Kaiser and Cai, 2012)

Categories	**Factors**
Seismic Event	Event magnitude, Rate of seismic energy release, distance to seismic source.
Geology	In situ stresses, Rock type, Beddings, Geological structures.
Geotechnical	Rock strength, Joint fabric, Rock brittleness
Mining	Mining induced static and dynamic stresses, excavation span, extraction ratio, mine stiffness, excavation sequence, installed rock support system, backfill, production rate.

Seismic energy, or rock falls by seismic quaking may cause damage in the form of rock bulking by fracturing and/or ejection of rock (Sousa, 2010). Distinct stages of damage are incurred to the underground excavation and the installed supports by each mechanism. The magnitude of damage depends on numerous factors, including:

- The stiffness of the country rock
- Magnitude of rock accelerations/velocities, induced stresses
- Excavation size, geometry, and orientation
- Effectiveness of the support system
- Geological structures.

Where observations and analytical methods are applicable, damage level can be determined. Rock mass classification is a useful analytical tool frequently used in tunneling projects for the assessment of rock mass quality and making a rough estimate of support requirements.

The chronological development of popular rock mass classification schemes and brief description of these schemes are given in Chapter 3. Application of support system is very restricted in dynamic loading environment, only fewer supports are suitable in this regard. Even the application of these support systems becomes restricted where severe ground conditions are encountered (Bawden, 2011).

High stresses in rock mass lead to the development of rock burst. In recent years, monitoring and predicting the rock burst events has been one of the most eagerly pursued topic in underground engineering. Unfortunately, till now a successful and mature monitoring system for rock burst prediction has not yet been developed (Liang, et al., 2013). There appears the need to develop appropriate computational tools that serve as methods of prediction and control of the rock burst (Shiyong, et al., 2010). These days, the studies on rock burst mechanism, its causes and preventive techniques are underway instead on past studies on the scale of phenomenon, regularity and rock burst hazard. Various theories, prediction tools and empirical relationships, such as fuzzy comprehensive evaluation, support vector machine (SVM), analytical principle and problems, artificial neural network, distance discriminant analysis, prior knowledge and the instability of rock masses, numerical simulation, laboratory integrated evaluation method, rock burst mechanisms, effects of sonic speed on rock burst location, seismological parameters, potential hydro-electric project site and source location methods have been suggested by the scholars (Dong, et al., 2013). A very useful tool, Finite Element Method (FEM) is developed for simulation of the entire unique process of rock instability failure (Li and Tang, 2015). FEM can also simulate and reproduce the entire process of rock failure from microscopic damage to macroscopic instability (Li, et al., 2014).

Numerical methods are frequently used to solve the problems encountered in intricate underground excavation activities. These methods provides researchers and engineers the most suitable tool to recognize and evaluate the failure mechanisms and predict the geotechnical risks associated with any underground excavation activity more effectively. In numerical modeling technique, when linear elastic models are used to analyze any underground opening, it does not offer full interpretation of the true stress state. Therefore, elasto-plastic models of the material are used to eliminate the inadequacy of linear elastic models. Hence, predicting likelihood of failure by finite element (FE) numerical modeling becomes essential (Abdellah, 2013).

1.3 Problem statement

The determination of mining-induced stress regimes as a function of overburden thickness, excavation sequence and pillar width between two parallel tunnels to assess the rock burst occurrence in the tunnels at a hydro-electric project site. The research is focused around the following question:

Is it possible to develop and implement an integrated engineering methodology to estimate mining-induced stresses as the function of overburden thickness, excavation sequence and pillar width between the parallel tunnels and simulate the excavation process using the finite element method, and use this methodology as a reliable predictive design tool for rock burst assessment in parallel tunnels?"

1.4 Objectives and Scope

The objectives of this research thesis are as follows:

- Rock mass characterization of potential hydropower project site
- Numerical modeling of parallel tunnels
- Assessment of rock burst potential
- Formulating suggestions and recommendations

The scope of this work is focused on hydroelectric power projects in northern areas of Pakistan. This work will help the engineers to minimize the rock burst hazards in tunnels and improve the work conditions thereby increasing the chances to complete the projects as soon as possible, reducing the overhead costs and damages due to the rock bursts.

1.5 Thesis Outline

Chapter 01 of this thesis provides an overview of the research. It discusses the general background of the study, the problem statement, the objectives and scope of the study.

Chapter 02 shows the literature review based on the objectives of this research study. The major focus is on: (i) history and general understanding of rock bursts; (ii) rock burst mechanisms; and (iii) rock burst assessment methods.

Chapter 03 discusses the general background of rock mass classification, its applications, advantages, drawbacks and commonly used classification schemes. In the end of the Chapter,

the rock mass of the potential hydro-electric project site is characterized as per Q-system and RMR.

Chapter 04 presents a potential hydro-electric project site of parallel tunnels, which was used to implement the research methodology. It discusses the general background of finite element numerical modeling, its application in rock burst analysis and numerical modeling of potential hydro-electric project site. 2D FE models of the parallel tunnels were constructed.

Chapter 05 presents an evaluation of rockburst prediction using the developed FE analysis model. In this chapter, rock burst analysis for different overburden thickness, excavation sequence and pillar widths is carried out.

Chapter 6 shows conclusions of this work. Suggestions and recommendations are also made to minimize the rock burst occurrence and future work.

At the end references are provided to properly acknowledge the research of different researchers.

Chapter 2 LITERATURE REVIEW

2.1 Rock Burst

It is quite clear from the available literature that the basic understanding of the rock burst phenomenon is not the same among the various researchers. For instance, the mechanism of rock burst described by Myrvang and Grimstad (1983) in Norwegian civil tunnels is quite different from the mechanism described by Ortlepp (1979) in deep-level underground mining condition. However, the common feature which is observed in all rock burst occurrences is the aggressive expulsion of rock pieces from the boundary of the excavation.

Per John (1983) defined the rock burst as a damage occurred in an abrupt or forceful manner in an underground excavation because of seismic activity. Broch and Sorheim (1984) stated that the rock burst in a metal mine or underground tunnel occurs in the geological condition of high stress area and is a dynamic phenomenon of rock crack and damage or rock ejection induced by the sudden release of rock mass stored elastic energy during the excavation process.

According to Brown (1988), the mechanisms by which rock bursts occur are sufficiently complex that it is even difficult to reach a consensus on the definition of a rock burst. Tan (1989) defined the rock burst as a dynamic geologic disaster triggered by progressive rock failure. Brady and Brown (1993) considered a rock burst as a sudden and violent expulsion of rock from the surrounding rock mass.

Blair (1993) classified the rock burst as a type of brittle failure which occurs mainly in the rocks around tunnels and is associated with a sudden large release of latent pressures. It occurs because of mechanical disturbance when the large quantity of strain energy accumulated within a rock mass is released suddenly, triggering a violent fracturing of the rock.

Ortlepp and Stacey (1994) applied the rock burst term to the excavation damage that results from a seismic activity. There is no concern for the type or magnitude of the seismic activity, the only requirement is that it must produce enough energy to release rock in a forceful manner or cause vicious damage to the excavation.

Palmstorm (1995) considered both rock burst and squeezing occur as instability caused by overstressing of continuous rock masses. Failures known as spalling, popping or rock burst arc caused by overstressing of brittle, massive rocks often at depths more than 1,000 m below surface. These failures can also be induced at shallower depth where high horizontal stresses or strongly anisotropic stresses are acting.

Shan and Yan (2010) defined the rock burst as the process of releasing elastic strain energy which is a dynamic failure phenomenon caused by human activity.

Shiyong, et al. (2010) characterized the rock burst as an explosion of a certain block causing a sudden rupture in the rock and is quite common in deep tunnels. It is an event that is caused by high stresses that occur in intact brittle rocks, located generally at great depths, during the excavation of an underground work.

Khanlari and Ghaderi-Meybodi (2011) considered the rock burst as one of the geotechnical hazards in the tunnels under high overburden and high in situ stresses. Rock burst is a typical geologic phenomenon caused by excavation in rock masses. In this phenomenon, the stress release and resultant explosion causes the damage to individuals or equipment.

Liu et al. (2011) stated that the rock burst is a kind of geological hazard triggered by the brittle rupture of surrounding rocks during unloaded excavation in high in-situ stress environments. It is basically accompanied by a sudden release of elastic strain energy and some other phenomena, such as slabbing, spalling, ejecting or throwing.

Panthi (2012) studied the tunnels passing through areas of high rock cover (overburden) and stated that these tunnels may be subjected to instabilities related to induced rock stresses. In relatively unjointed and massive strata, if the rock mass strength is less than the induced stresses the instability may be mainly associated with rock spalling or rock bursting. On the other hand, if the rock mass is weak, schistose, sheared, deformed and thinly foliated/bedded; squeezing is the most likely scenario.

Dong, et al. (2013) considered the rock burst as a dynamic instability process that occurs in adjacent rock mass of an underground excavation located in high in-situ stresses and triggered by the fierce release of stored energy in the rock. Rock burst problem arises during the excavation of an underground space and it can occur in the form rock fall or rock slices or ejection of rock pieces, sometimes with a crack sound.

Yu et al. (2015) defined the Rock burst as a dynamic instability phenomenon associated with bursting loose, stripping, ejection, and even catapulting of rocks, where these effects are caused by the sudden release of accumulated elastic strain energy from brittle surrounding rocks during the excavation of underground caverns under high stress.

Kabwe and Wang (2015) stated that rock burst is a phenomenon that results from a seismic event which is caused by mining activity and it causes damage to underground excavations.

Wen et al. (2016) defined the rock burst as a dynamic phenomenon with sudden severe damage, throw-out of large quantity of rock and loud sound in the surrounding rock of roadway or working face, which is induced by instantaneous release of elastic deformed energy of the surrounding rock and occurs during the mining process.

Rock burst incidences in underground excavations have been stated from several countries for decades, and it seems like there are diverse perceptions of rock bursting (Ortlepp and Stacey, 1994). Different researchers have stated different eras for the record of first rock burst e.g. Jiang et. al. (2010) stated the first documented rock burst in 1938 in a coal mine in England, Balke and Hedley (2004) recorded the evidence of first rock burst in early 1900s in South African Mines, and Guo et. al. (2003), Shan and Yan (2010), Wen et. al. (2016) documented the first recorded rock burst almost 280 years ago in 1738 in a British tin mine. Later, several reports of rock burst from all over the world came to sight.

Rock bursts are frequent in South Africa, largely in gold mines. In 1975, 680 rock bursts occurred majority of which was recorded in gold mines due to greater depths causing death of 73 persons (Yu, et al., 2015). The number of rock burst and degree of damage because of rock burst in China is very alarming. In China, rock burst occurred in 32 coal mines in 1985, and the number increased up to 142 in 2012. During the period of 2006–2013, 35 rock bursts were experienced in nine coal mines, 300 individuals died, and about one thousand persons were injured in these sad accidents (Wen, et al., 2016). During the construction of Jinping II Hydropower station in China, a 120 million Yuan worth tunnel boring machine (TBM) was buried forever and construction was stopped due to a violent rock burst (Yu, et al., 2015). Rock burst is now widely accepted as a major geological problem generally faced during underground excavation of mines, tunnels and caverns etc. under high in-situ stresses (Shan & Yan, 2010).

The safety of personnel working in an environment with a probability of rock burst occurrence is always at risk as well as it poses a significant threat to the performance of tunneling indentures. The number of rock bursts reported has increased with the increase in tunneling depths (Ortlepp and Stacey, 1994; Lu, et al., 2008; Kabwe and Wang, 2015). Likely effects of rock burst may include damage and deformation of tunnel periphery, injuries and deadly accidents, damage or loss of equipment, production and construction interruptions, increased cost of production and construction, damage to supports, distortion of working face and roadways, excavation collapse in worst condition and even ground surface collapse that can induce local shaking as earth quake (Prochazka, 2004; Sharan, 2007; Liu, et al., 2011; Panthi, 2012; Dong, et al., 2013; Yu, et al., 2015).

2.2 Rock burst Mechanism

Since the record of first rock burst, numerous scholars have conducted research on rock burst. Many researchers have proposed their theories about the mechanism of rock bursts but none of those is accepted yet uniformly as the rock burst is an intricate dynamic instability (Lu, et al., 2008). The main source of rock bursts in hard rocks is generally the strain energy and the processes involved in this phenomenon are generally static in nature (Gao, et al., 2008). However, the accrual of strain energy is an essential condition for rock bursts but it is not an essential and enough condition. The driving force behind most of the rock bursts is the combination of local energy and transfer energy (Yu, et al., 2015). Thus. an external source of disturbance is also required for a rock burst (Lu, et al., 2008).

More and more rock engineering projects are being constructed at greater depths with high stresses (Dong, et al., 2013). Elastic strain energy is easily accumulated to elevated levels at higher depths (Liu, et al., 2011). So, with the increase in mining depth, the probability of rock burst also increases (Zhang and Wang, 2007; Duo, et al., 2009; Kabwe and Wang, 2015). It is, hence, crucial to better understand the mechanism of rock bursts. Sharan (2007) classified the rock bursts into two major types: crush type, and the shear type.

The crush type rock bursts occur because of the stress concentration also known as strain bursts and deformation of underground excavations however the shear type rock bursts occur due to the existence of geological structures known as fault slip bursts.

Most of the seismicity that occurs close to the mining activity is due to unexpected mining induced stress changes. Both, the structural geology of the area and excavation activities, play

key role in the onset of rock burst events. (Malek, et al., 2009). The locations with elevated levels of stress concentration along with elastic stored energy are mostly prone to rock bursts. Mining induced stress is a dynamic feature for rock burst incidence (Wen, et al., 2016).

Rock bursts occur often during the process of excavation and are associated with the rock fracturing. Generally, rock bursts involve two situations for their manifestation:

- a stress greater than the rock strength, and
- physical properties of the rock to accumulate energy for abrupt break.

The size of the underground excavation also affects the rock burst occurrence. The larger the size of excavation, the riskier it will be. Induced seismicity can also trigger rock bursts e.g. faulty procedures of mining. Other sources of rock bursts include the existence of joints, dykes, or faults etc. (Dong, et al., 2013).

Shan and Yan (2010) described the rock burst as a phenomenon of dynamic failure in rock because of human activity. After laboratory testing and comprehensive study of the rock burst, they believed that accumulation and release of energy causes the high stress rupture. They divided the rock burst process into three phases:

- energy accumulation,
- formation and propagation of micro-cracks,
- crack coalescence and burst.

Energy accumulation: Virgin rock mass, when undisturbed, is in a balanced state of stress. The excavation process relieves the radial stresses and surrounding rock tends to deform towards the excavated space and some of the strain energy is released. The stresses around the periphery of the excavation redistribute, thereby, increasing the tangential stress that leads to the accumulation of energy around the periphery of the opening.

Formation and propagation of micro-cracks: High stresses start to progress at the ends of micro cracks formed due to the stress redistribution. If these stresses surpass the rock strength, the stored energy will be released by propagating the crack. During this process, these micro cracks intercept with other cracks and develop into macro cracks.

Crack coalescence and burst: The crack propagation carries on and a point comes when elastic strain energy is transformed into the kinetic energy that expels the rock mass from its position and causes a rock burst.

Kabwe and Wang (2015) classified the rock burst into three categories:

- Strain bursts
- Pillar bursts
- Fault slip bursts

Strain bursts: These type of rock bursts are triggered by high levels of stress around the periphery of mine openings that surpass the rock strength.

Pillar bursts: These are severe type of rock bursts and involve hundreds of tons of rock material, because of the complete support pillars collapse.

Fault slip bursts: These are caused by sudden slippage of rock along any geological structure like fault. It occurs in the same manner as the earthquake.

The rock burst damage may be in the form of bulking, ejection, or rock falls (Kaiser and Cai, 2012). Each mechanism of rock burst has different magnitude of damage on the opening and the installed supports.

Ortlepp and Stacey (1994) gave a detailed insight to the mechanism of rock bursts in tunnels and shafts. Even though, the complete understanding of the cause of seismic incident is not essential to understand the rock burst issues in underground working environments, it is important to recognize that seismicity and rock burst are not essentially the identical events. Different authors have defined seismicity in separate ways. It can be defined as the response of rock material to distortion and breakage (Kabwe and Wang, 2015). Thus, it is advantageous to understand the main categories of source mechanisms to demonstrate in what manner impulsive loading or stresses on an excavation can differ in intensity and nature. The major source mechanisms are listed as under:

- Strain bursting
- Seam buckling
- Face crushing
- Shear rupture
- Fault/Slip

A classification of seismic event sources is suggested in Table 2.1 based on Ortlepp (1992) to differentiate these categories depending upon the mechanism and scale of seismic activity.

Table 2.1: Seismic event source mechanisms and their magnitudes (After Ortlepp, 1992)

Seismic Event	**Postulated Source Mechanism**	**First Motion from Seismic Records**	**Richter Magnitude**
Strain-bursting	Superficial spalling with violent ejection of fragments	Usually undetected; could be implosive	- 0.2 to 0
Buckling	Outward expulsion of pre-existing larger slabs parallel to opening	Implosive	0 to 1.5
Face crushing	Violent expulsion of rock from tunnel face	Implosive	1.0 to 2.5
Shear rupture	Violent propagation of shear fracture through intact rock mass	Double-couple shear	2.0 to 3.5
Fault-Slip	Violent renewed movement on existing fault	Double-couple shear	2.5 to 5.0

The mechanism of first three seismic event sources is different from that of last two as it is observed that the cause and damage positions for the initial three seismic event mechanisms are possibly coincident that is, the source and damage are in the same rock. For instance, strain bursting is observed exactly at the excavation periphery and it is strongly influenced by the geometry of the excavation and accumulation of stresses around the periphery. But the other two mechanisms characterize shear failure of the rock mass on some "plane", and resultant shear failure region can extend up to thousands of feet.

There are insufficient available conclusive studies about the damage mechanisms of rock burst. Ortlepp (1992) classified the distinct sorts of damages caused by rock bursts and used this classification to treat the rock burst damage. Distinct types of rock bursts depending upon the damage mechanism are listed as under:

- Strainbursts
- Buckling
- Ejection
- Arch collapse

Strainbursts are perhaps the most commonly observed damage mechanism in tunnels. The distinctive characteristics and geometry of a strainburst are shown in Figure 2.1. The rock fragments are usually sharp edged thin plates and are violently expelled from the rock surface.

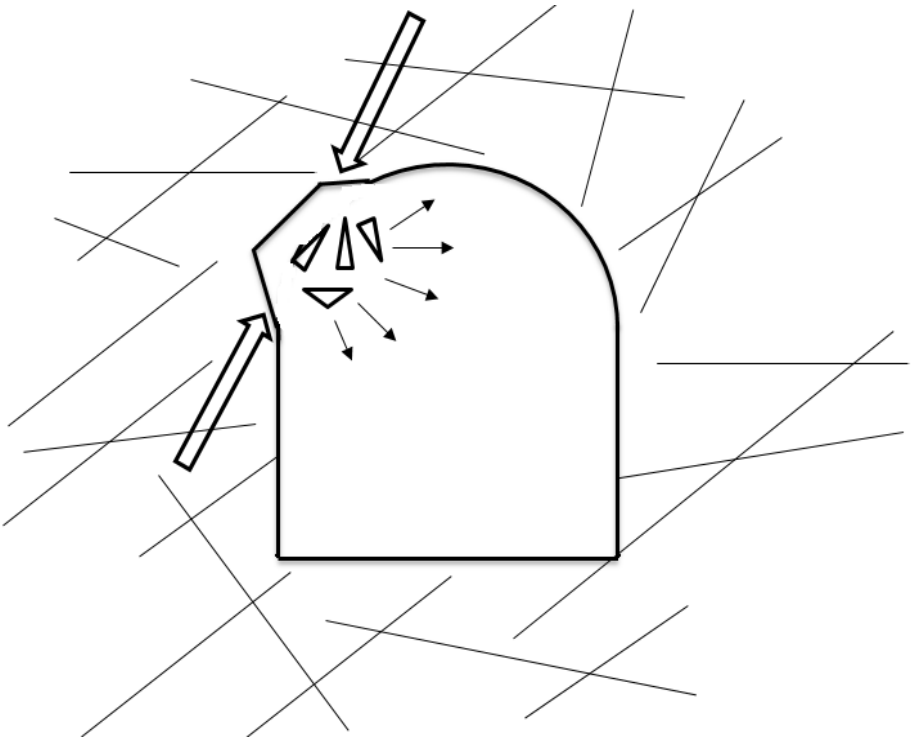

Figure 2.1: Strainburst: Detachment of spalls because of localized stress concentration.
(Modified after Ortlepp and Stacey, 1994)

The safety concern that is related to strain bursts is mainly due to the edges of the rock fragments that are very sharp and the ferocity of ejection. In some cases, the rock fragments can be dangerous due to their sizes or masses as well. The locations from which these rock fragments may be expelled will differ, depending on; (Broch and Sorheim, 1984)

- the in-situ stress field orientation, and
- the profile geometry

Most commonly, strain bursting occurs behind the working face at a distance approximately equal to half a diameter to three times diameter of the tunnel, but it may occur from the face as well. There are more chances of strain bursting in a massive rock than a fractured or jointed rock mass. The strain bursting occurrence increases as the strength of the rock increases (Broch and Sorheim, 1984). In the similar rock, the likelihood of strainbursting is greater in a mechanically excavated tunnel as compared to D and B excavated tunnel. Stacey and Thompson (1991) reported a case of strain bursting in a tunnel that was excavated with

the help of roadheader, but there wasn't any report of such incident in a tunnel in line within the same rock excavated by conventional drill-and-blast methods. The blasting de-stresses the skin of the adjacent rock mass resulting in an environment much less favorable for strain bursting. Although, strain bursting is expected to be more severe in brittle rock masses but it doesn't only occur in brittle rock environments. Stacey (1989) estimated that fracturing starts in tunnels as soon as ground stress approaches to 15% of uniaxial compressive strength of the rock, thus causing a possibility for strain bursting to occur. Strain bursting environments cause substantial cutting problems for machine excavation techniques (Stacey, 1989) (Stacey and Harte, 1989). It may be a prime cause to decrease the tunnel progress rates significantly (Myrvang and Grimstad, 1983; Sperry and Heuer, 1972; Binder, 1978).

Buckling is mostly observed in laminated or diagonally anisotropic rock masses. However, it is not compulsory that buckling will only occur in the sidewalls. It can occur at anyplace around the opening periphery where the inclination or orientation of geological structure is satisfactory for buckling activity. Buckling in a laminated or transversely anisotropic rock is shown in Figure 2.2.

The main energy source for buckling damage mechanism is the strain energy that is stored in the laminations of rock. However, the seismic wave whose source can be located somewhere away from the site of damage can deliver the additional energy. Rock bursts with scales of 1.8 and 2.3 are thought to have taken place due to the buckling at Strathcona Mine in Craig Haulage Drift in Canada (Semadeni, 1991).

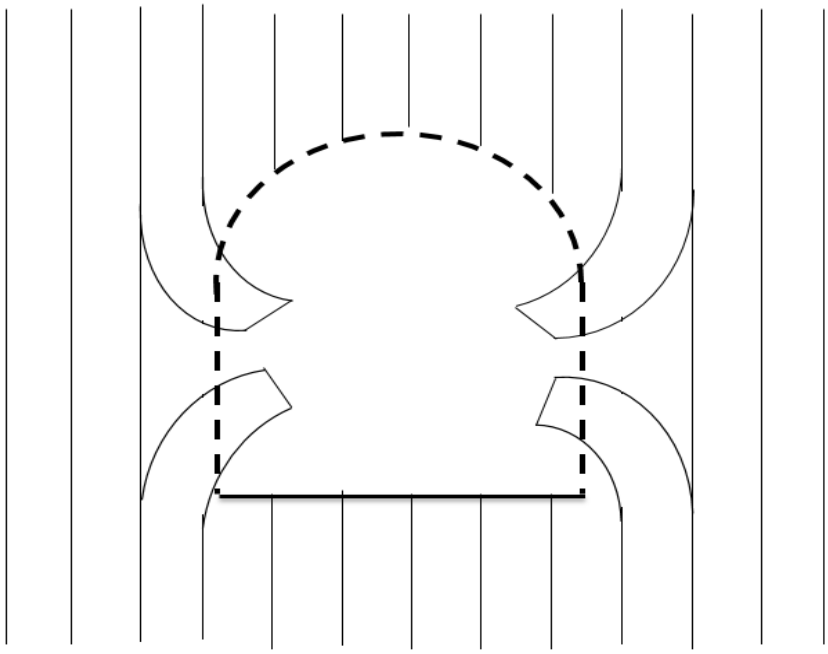

Figure 2.2: Buckling: Rock bursting in a laminated or transversely anisotropic rock.
(Modified after Ortlepp and Stacey, 1994)

Ejection is basically the expulsion of rock mass from the periphery of the tunnel directionally coupled with the passing energy-wave. Pre-existing joints and/or induced fractures dictate the movement and geometry of ejected rock blocks. The mechanism of ejection is demonstrated in Figure 2.3.

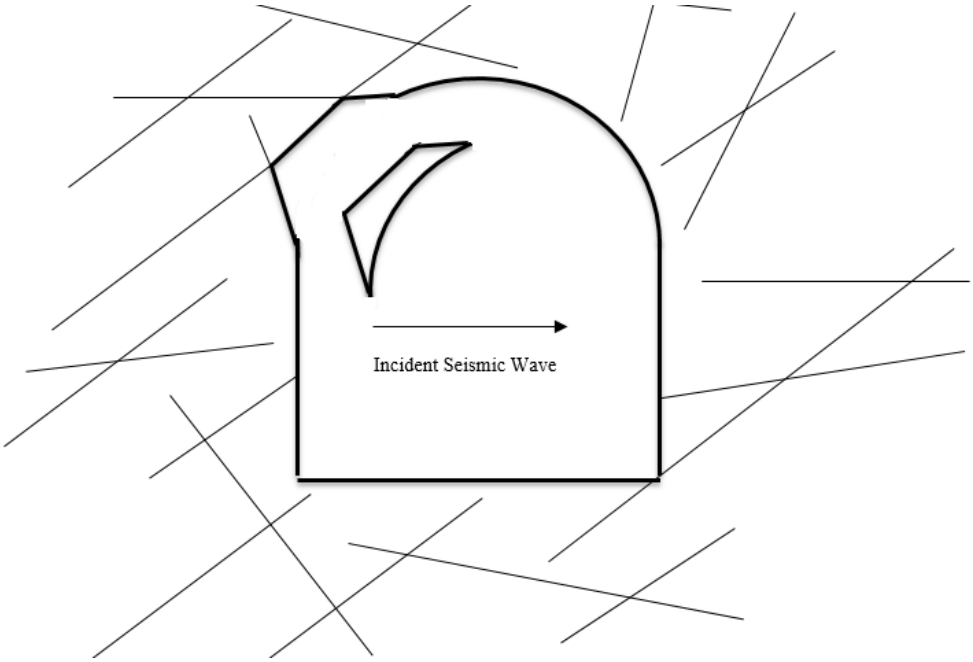

Figure 2.3: Ejection: Expulsion of a block of rock defined by fractures or joints.
(Modified after Ortlepp and Stacey, 1994)

The energy required for this sort of rock burst comes from any seismic incidence, whose focus may be present away from the region where damage has occurred. The location of rock burst source and resultant damage are not coextensive as it were in strain bursting and buckling type rock burst. The damage because of the ejection type rock burst is dependent upon;

- scale of seismic event, and
- the distance between the source and damage location.

The velocity of the ejected material is estimated up to 10 m/s. Ejection type rock bursts mainly occur in mining tunnels as the source of such rock bursts is seismicity.

Arch collapse is a sort of ejection type rock burst with the difference that the main driving force involved in arch collapse in not a seismic event, rather it is due to the gravity. Additional acceleration can be provided by seismicity to overcome the shear strength of surfaces. Such rock burst occurs due to the existence of pre-existing geological structures and/or induced fractures. This helps the gravity to move large wedges or blocks of rock. The mechanism of arch collapse is shown in Figure 2.4.

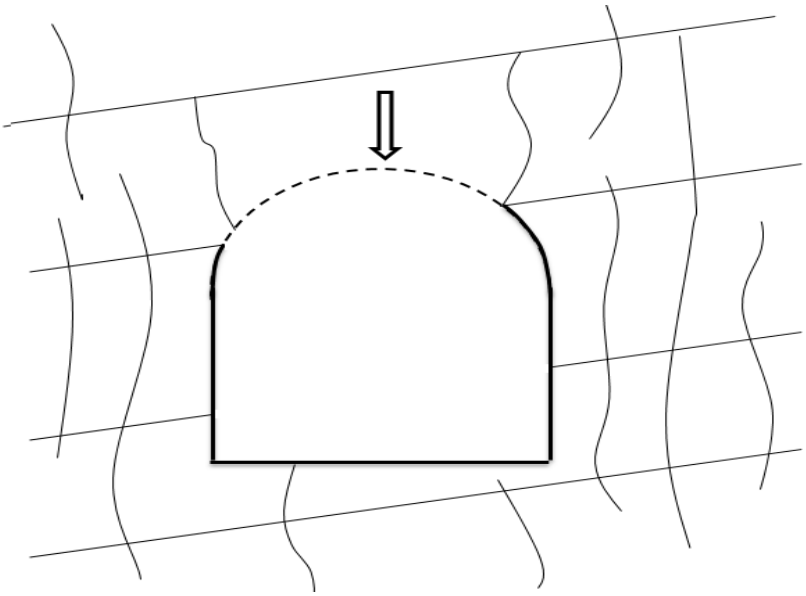

Figure 2.4: Arch Collapse: Collapse of tunnel roof due to gravity enhanced by shear wave. (Modified after Ortlepp and Stacey, 1994)

Malmgren (2005) classified the rock bursts into two categories

- self-initiated rock bursts, and
- remotely triggered rock bursts

Self-initiated rock bursts occur due to the stress redistribution that result in stress concentration close to the periphery of the excavation. When these stresses exceed the rock strength, rock fails in an unbalanced manner. Rock burst can also take place due to the structural instability as observed in buckling of rock slab or column. This factor is independent of rock strength.

Remotely triggered rock bursts are generated by high scale seismic events. These type of rock bursts occur in hard rock mines after the mining activity of significant area and/or where the geological structures intersect stopes and/or sill pillars. Rock mass fracturing and structural instability occur because of large ground vibrations and dynamic stresses.

It is important to note that strain bursting is the most susceptible source of rock bursts observed in civil engineering projects, other mechanisms are most liable to occur in mining engineering projects. It is also observed in some case histories that rock bursting is likely to occur with mechanical excavation as compared to drill-and-blast excavation within the same rock (Ortlepp & Stacey, 1994).

2.3 Rock burst Assesment

There are various methods to monitor, predict and analyze the rock burst phenomenon but none has proved successful in all sort of conditions (Mansurov, 2001; Sharan, 2007; Hu, et al., 2011; Liang, et al., 2103; Yu, et al., 2015). Zienkiewicz and Taylor (1989) considered the finite element method as the most appropriate method to analyze such type of complex problems. Bardet (1989) used this method for rock burst analysis as a buckling problem. In geomechanics, the finite element analysis has some limitation due to the substantial extent of rock or soil material (Sharan, 1992). Viladkar, et al. (1994) reported numerical instability if infinite elements are used for an elasto-plastic analysis. Sharan (1989; 1993) developed a method to eliminate the problems related to significant extent of material and infinite elements. This method uses multi-directional elastic supports along the truncation boundary during finite element analysis. This approach was effectively used to analyze fractures in elasto-plastic condition (Sharan, 2000) and to analyze underground openings in elastic-brittle-plastic condition (Sharan, 2003). Tang (2010) used acoustic emissions to monitor the cracking and to evaluate the potential of a rock for rock burst.

Panthi (2012) stated a simple rule of thumb used by Norwegians to predict the likelihood of rock burst occurrence. As per this rule, if a tunnel overburden exceeds about 500 m, the tunnel is susceptible to experience spalling or rock burst.

Khanlari and Ghaderi-Meybodi (2011) used following four criteria to predict the rock burst occurrence in critical sections of a tunnel:

- Strain energy,
- Rock brittleness,
- Seismic energy, and
- Tangential stress criterion

Vertical stresses on the tunnel are calculated by following relation:

$$\sigma v = \gamma(Z) \qquad (2.1)$$

σ_v = vertical stress (MPa),

γ = unit weight of rock mass (MN/m3),

Z = tunnel depth (m).

Many researchers have proposed that the accumulated strain energy in the rock mass is the major source behind the rock burst occurrence. But there are other external factors as well. Blair (1993) stated different disturbance factors in tunnel construction e.g. explosion vibration, stress influence of any nearby rock bursts, earthquakes etc. Here is brief discussion of criteria used by Khanlari and Ghaderi-Meybodi.

Elastic strain energy criterion:

Investigation reveals that the occurrence of rock burst could be predicted and scaled by the so-called potential energy of elastic strain, SED, that is given by:

$$SED = \frac{\sigma c^2}{2Es} \qquad (2.2)$$

Where, σc is the uniaxial compression strength (MPa), Es is the unloading tangential modulus (MPa). In the opinion of Polish experts if:

SED < 40 kJ/m3, then the rock burst hazard is low;
40 ≤ SED < 100 kJ/m3, then the rock burst hazard is moderate;
100 ≤ SED < 200 kJ/m3, then the rock burst hazard is strong;
SED ≥ 200 kJ/m3, then the rock burst hazard is very high.

Rock brittleness criterion:

Rock brittleness is given as:

$$B = \frac{\sigma_c}{\sigma_T} \qquad (2.3)$$

Where, σ_c is the uniaxial compression strength (MPa), σ_T is the tensile strength of the rock (MPa). Experimental study and in situ investigation show that:

B > 40, then no rock burst;
B = 40 - 26.7, then weak rock burst;

B = 26.7 - 14.5, then strong rock burst; and

B < 14.5, then violent rock burst.

Tangential stress criterion:

The criterion of tangential stress is stated as:

$$Ts = \frac{\sigma_\theta}{\sigma_c} \qquad (2.4)$$

Where, σ_θ is the tangential stress in rock mass surrounding the openings or stopes (MPa) and σ_c is the uniaxial compressive strength of rock (MPa). According to Wang and Park (2001), the rockburst tendency can be evaluated using Ts criterion as presented below.:

Ts < 0.3, then no rock burst;

Ts = 0.3-0.5, then weak rock burst;

Ts = 0.5-0.7, then strong rock burst; and

Ts > 0.7, then violent rock burst.

Rock burst analysis showed that the tunnel sections with large overburden and weak rock mass conditions are more likely to experience rock burst because of high in situ stresses and tangential stresses.

Martin, et al. (1999) reviewed different underground openings and showed that the brittle failure initiates when the damage index exceeds 0.4. Damage index is the ratio of maximum tangential stress at the boundary to UCS determined in laboratory. Martin and Chandler (1994) showed that most of the cohesion of the rock mass is lost before the mobilization of peak friction during the brittle failure process. Martin (1997) stated that the maximum rock mass strength at the periphery of the opening is almost 0.4 times the laboratory determined compressive strength.

Liu, et al. (2011) reviewed different rock burst prediction and control methods, such as Erlang mountain method, Tao Zhenyu criterion, Qinling method, Hou Faliang criterion, Norway Barton criterion, Russense criterion, Turchaninov criterion, Kidybinski method and Hoek criterion, and present a rock burst classification as given in Table 2.2.

Table 2.2: Classification of rock burst (After Lipeng Liu et. al., 2011)

Grade of Rock burst	UCS/Maximum stress	Failure depth (m)
Slight	4-7	< 0.5
Moderate	2-4	0.5-1.0
Intensive	1-2	1.0-2.0
Extremely intensive	<1	> 2.0

Dong, et al. (2013) reviewed different criteria laid down by various researchers and compared those criteria. A comparison of different criteria based on stresses is given in Table 2.2.

Table 2.3: Rock burst assessment criteria considering the stresses only (After Dong, et al., 2013)

Scholar	Criteria of Rock Burst	Activity
RUSENSES	$\sigma_\theta / \sigma_c < 0.20$	No rock burst activity
	$0.20 \leq \sigma_\theta / \sigma_c < 0.30$	Light rock burst activity
	$0.30 \leq \sigma_\theta / \sigma_c < 0.55$	Medium rock burst activity
	$\sigma_\theta / \sigma_c \geq 0.55$	Violent rock burst activity
HOU et al	$\sigma_1 / \sigma_c < 0.30$	No rock burst activity
	$0.30 \leq \sigma_1 / \sigma_c < 0.37$	Light rock burst activity
	$0.37 \leq \sigma_1 / \sigma_c \leq 0.62$	Medium rock burst activity
	$\sigma_1 / \sigma_c > 0.62$	Violent rock burst activity
WANG et al	$\sigma_\theta / \sigma_c < 0.30$	No rock burst activity
	$0.30 \leq \sigma_\theta / \sigma_c < 0.50$	Light rock burst activity
	$0.50 \leq \sigma_\theta / \sigma_c \leq 0.70$	Medium rock burst activity
	$\sigma_\theta / \sigma_c > 0.70$	Violent rock burst activity
HOEK	$\sigma_\theta / \sigma_c = 0.34$	Light stripping
	$\sigma_\theta / \sigma_c = 0.42$	Violent stripping
	$\sigma_\theta / \sigma_c = 0.56$	More lining
	$\sigma_\theta / \sigma_c = 0.70$	Violent rock burst
TAO	$\sigma_c / \sigma_1 > 14.5$	No rock burst activity
	$5.5 < \sigma_c / \sigma_1 \leq 14.5$	Light rock burst, with light sound
	$2.5 \leq \sigma_c / \sigma_1 < 5.5$	Medium rock burst, with crack sound
	$\sigma_c / \sigma_1 < 2.5$	Violent rock burst, strong crack sound

TURCHANINOV	$(\sigma_\theta+\sigma_L) / \sigma_c \leq 0.3$	No rock burst activity
	$0.3 < (\sigma_\theta + \sigma_L) / \sigma_c \leq 0.5$	Rock burst probably
	$0.5 < (\sigma_\theta + \sigma_L) / \sigma_c \leq 0.8$	Rock burst surely
	$(\sigma_\theta + \sigma_L) / \sigma_c > 0.8$	Violent rock burst activity
BARTON	$\sigma_c / \sigma_1 = 5-2.5$ and $\sigma_c / \sigma_1 = 0.33-0.16$	Medium rock burst
	$\sigma_c / \sigma_1 < 2.5$ and $\sigma_c / \sigma_1 < 0.16$	Violent rock burst

Rock burst problem is site-specific and it depends upon several factors such as in-situ stresses magnitude and direction, rock mass strength, tunnel geometry and excavation methods. Liu et al, (2011) used Phase2 software for finite element modeling of the rock burst using the generalized Hoek-Brown criterion given by (Hoek, et al., 2002) and showed that:

- Drill and blast method releases some of the strain energy accumulated in the rock mass as compared to TBM method. Therefore, the rock bursts with D and B method are of low grade while rock bursts with TBM method are of high grade.
- Tunnel geometry have varying effect on stress redistribution of the rock mass.
- Small distance between parallel tunnels have higher effect on each other because of the influential extent of the maximum principal stress.

The rock burst characteristics will be different depending upon the different geological conditions.

2.4 Summary

Rock burst is highly undesirable phenomenon in underground excavation because of the possible effects of a rock burst. Therefore, it is critical to comprehend the rock burst phenomenon, concentrating on the pattern of manifestation so that these incidences can be evaded and/or managed, saving lives and costs. Moreover, due to the intricacy of the mechanism of rock burst and its prediction, study on the mechanism and prevention of rock burst is comprehensively required.

In this chapter, the history and general understanding of rock bursts, its effects, rock burst mechanism and assessment techniques are reviewed. The assessment techniques are mostly case studies based and there is a need to develop a generally accepted rock burst assessment method in future.

Chapter 3 ROCK MASS CHARACTERIZATION

3.1 Introduction

To predict the behavior of a rock mass, it is often designated some unique representation or a number based on comparable properties and classified into different sets because of characterized relationships. The system of representing and classifying rocks is called rock mass classification or rock mass characterization (Bieniawski, 1989). Rock mass is defined as a collection of rock material isolated by discontinuities, generally by joints, faults, bedding planes, etc. Bedding planes, faults and dyke invasions are not that common if compared to joints in the rocks and, therefore, are studied separately (Bieniawski, 1993). This classification system provides a guideline to place the rock masses in suitable classes. It is, however, misleading to use these classification systems directly in their original form as they are developed for a particular rock mass or specific purpose. That is why rock engineers try to modify these systems or develop new ones (Aydan, et al., 2014).

The rock mass characterization is intended to appropriately impart the evaluated rock mass properties and ought not to be taken as a substitute to comprehensive engineering design strategies. These classification schemes are not appropriate to use in detailed design of complex subsurface openings, particularly (Bieniawski, 1989). For such type of use, there is a need to further develop these classification systems. These systems were intended to aid in engineering design, and were not designed as an alternative to observations made in the field, measurements, analytical designs, and final decision (Bieniawski, 1993).

Characterization schemes might be valuable devices for evaluating the requirement for excavation support at the planning stage, especially for tunnels in jointed and hard rock masses. However, there are various limitations that ought to be considered when that system will be utilized for other rock masses. So far, such limitations have not been quite examined in available research work (Palmstorm & Broch, 2006).

These systems provide a basic outline for design purposes and are progressively utilized as a part of both, the empirical and the numerical design approaches, as the computing power moves forward. This ought to be utilized as a part of other design methods to develop a compatible design with site geology and design objectives. Practically, rock mass classification systems have aided considerably in systematic design of various engineering projects, particularly in underground excavations (Hoek, 2007).

3.2 Applications of rock mass classifications

These rock mass classification systems give a premise to understand the rock mass behavior, and narrate the site to site practices in different ground environments. During early design stages of any project, complete information regarding rock mass properties is mostly inaccessible. Hence rock mass classification provides aid at this level to understand the rock mass pattern and behavior. It provides necessary information to estimate the support requirements for any rock mass using its strength, composition and deformation properties etc. as well as it demonstrates the relevance and importance of that information (Bieniawski, 1989).

Bieniawski (1993) enlisted following objectives of rock mass classification:

- To recognize the most important parameters affecting the rock mass behavior
- To classify a rock formation into various rock mass groups of variable qualities
- To give a premise to understand the attributes of individual rock masses in a rock
- To extract numerical information for excavation design purposes
- To suggest the support requirements for underground openings
- To give a general premise for correspondence amongst engineers and geologists
- To relate the site to site experiences in different rock conditions

Rock mass classification systems are also applied in combination with numerical modeling techniques, especially in preliminary design stages when the available data is very limited. Using the rock mass classifications, the strength and the deformation characteristics of the rock mass can be calculated and used in numerical modeling techniques to analyze the stability of the opening, failure pattern, deformations and factor of safety etc. Rock mass classification systems are successfully implemented in underground mining projects and slope stability analysis (Herbst and Konietzky, 2012; Chakraborti, et al., 2012).

3.3 Benefits of Rock Mass Classifications

The benefits of rock mass classifications are listed as under; (Bieniawski, 1989; Bieniawski, 1993; Hoek, 2007).

- Rock mass classification improves the site investigation quality as it requires a systematically identified and quantified input data.

- A balanced, quantified measurement and classification is more reliable than a qualitative and personal assessment.
- The main characteristics of individual rock mass types of any formation can be estimated.
- Classification outcomes in numerical data for the design purpose and permits improved engineering judgment and more effective correspondence on an engineering project.
- Relationships between the quality of rock mass and its mechanical attributes have been proposed and are applied to calculate its mechanical attributes and its swelling or squeezing behavior.

3.4 Drawbacks of Rock Mass Classifications

The major drawbacks of these systems arise when; (Bieniawski, 1993)

- Rock mass classifications are used as an ultimate design outcome ignoring other design methods.
- Single classification scheme is used without comparing the results with any of other classification schemes.
- Rock mass classification is used without having sufficient input data.
- Classification systems are used without complete understanding of the limits and the conservative nature of the database used for their development.
- Some people also believe that the earth resources cannot be designated by a single number.

3.5 Parameters required for classification

The intact rock mass is considered as continuous while a jointed or fractured rock mass is taken as discontinuous. Whenever an engineering project is designed in a rock mass, its engineering properties should be given due consideration. To assure the stability of the rock mass, different parameters of varying significance are considered to describe the rock mass reasonably. The important parameter that are used for the classification and description of a rock mass are listed as under; (Bieniawski, 1993)

- Intact rock mass strength (UCS, Young's Modulus etc.)
- Rock quality designation (RQD)

- Characteristics of rock discontinuities (orientation, spacing, aperture size, infilling etc.)
- Groundwater characteristics (pressure, flow)
- In-situ stresses
- Main geological structures (folds, faults etc.)

3.6 Major types of rock classification systems

These characterization systems can be divided in to two groups qualitative and quantitative based on the mode of classification. Qualitative classification systems are descriptive ones. These systems include Rock load, Geological or Geotechnical Strength Index (GSI) and SIA 199 (Schweizerischer Ingenieurund Architekten-Verein). Quantitative classification systems include Q-system, Rock Mass Rating (RMR), Rock Structure Rating (RSR) and Rock Quality Designation (RQD) which quantify the rock mass with numerical values.

These systems can also be categorized on the basis of the purpose for which these systems are applied such as Q-system and RMR system are used to assess the stability of the opening. Q-system is also used to estimate the support requirements of the excavation e.g. bolt spacing, liner thickness etc. RMR system can also be used for this purpose but with some modifications. SIA 199 is used to determine the support and excavation classes. GSI is applied when we only need to estimate the engineering design parameters.

3.7 Commonly applied rock mass classifications

Rock mass classifications have been evolving since 1879 when Ritter developed an empirical method to design a tunnel and its support requirements (Hoek, 2007). Most of classification systems (Bieniawski, 1968; Wickham, 1972; Barton et al., 1974; Bieniawski, 1973, 1989) have their origin from the projects of civil engineering (Hoek, 2007). The most widely applied classification systems are RQD, RMR, GSI and Q systems to assist in designing the underground excavations.

3.7.1 Rock Quality Designation (RQD)

Rock quality designation (RQD) was developed by Deere in 1967 (Deere and Deere, 1988). It is a technique for logging sound rock core drilled to compute and evaluate the proportion of intact rock in a core run. RQD is a numerical technique for assessing rock quality and is broadly utilized as one of the parameters in other more quantitative rock characterization systems. RQD is defined as percentages of intact core pieces longer than 10 cm in the total length of a core sample having core diameter of 54.7 mm, as shown in Figure 3.1 (Hoek, 2007).

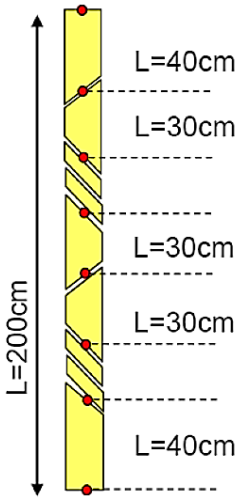

Procedure to calculate the RQD for the example given in figure 3.1 is as follows:

$$RQD = \frac{\Sigma \text{ length of core pieces 4 inches or greater}}{\text{Total core length}} 100\% \qquad (3.1)$$

$$RQD = \frac{40+30+30+30+40}{200} 100\%$$

$$RQD = 85\%$$

Figure 3.1: Core run having different pieces of intact length (Modified after Hoek, 2007)

Number of discontinuities which are visible on exploration adits or the outcrops in a unit volume, for clay-free rock masses, are also used to estimate the RQD as given below:

$$RQD = 115 - 3.3\ Jv \qquad (3.2)$$

Where Jv is the volumetric joint count and is defined as the total number of joints in a unit length. RQD is a borehole orientation dependent index. RQD characterizes the in-situ quality of the rock mass. Rock mass quality as per RQD classification is shown in Table 3.1.

Table 3.1: Rock mass quality classification according to RQD (After Deere and Deere, 1988)

RQD	< 25	25 – 50	50 – 75	75 – 90	90 – 100
Rock Mass Quality	Very poor	Poor	Fair	Good	Excellent

However, RQD has some limitations in its application.

- It doesn't provide the true picture of rock mass quality because it only accounts for the degree of fracturing and does not consider the rock mechanical properties.
- It doesn't provide a good estimate of the fracturing extent of the rock mass as well because it is borehole orientation dependent.
- It cannot consider the joints lengths as well which are under consideration (Palmstorm & Broch, 2006).

3.7.2 Rock Mass Rating (RMR)

Rock mass rating (RMR) was developed by Bieniawski in 1973 (Bieniawski, 1989) to evaluate the tunnel's stability and its support requirements. It has been improved and refined successively since then by examining more and more available case histories. The basic advantage of RMR system lies in the simplicity of its input parameters. These parameters are related to the mechanical properties of the rock mass and geometry of discontinuities. To classify a rock mass, RMR system includes the rock mass information regarding: (Bieniawski, 1989)

- RQD
- Rock strength
- Discontinuity condition
- Discontinuity spacing
- Groundwater
- Discontinuity orientation

These parameters of the rock mass are given some numbers depending upon the nature of these parameters and their summation gives the rock mass rating. Bieniawski (1989) classified the rock masses in to various categories as given in Table 3.2.

Table 3.2: Rock mass quality according to RMR (After Bieniawski, 1989)

RMR value	Rock Class	Rock Quality
81-100	I	Very good rock
61-80	II	Good rock
41-60	III	Fair rock
21-40	IV	Poor rock
Less than 20	V	Very poor rock

RMR values are used for the estimation of the stand-up time for the tunnel, maximum stable span and the strength parameters of the rock mass for the Mohr-Coulomb criterion. However, RMR system is conservative one and can estimate greater support requirements (Bieniawski, 1989). RMR system was mostly based on tunneling in competent rocks case histories so its application in weak rocks is somewhat questionable (Singh and Geol, 1999).

3.7.3 Rock Tunneling Quality Index (Q-System)

To determine the rock characteristics and support requirements for a tunnel, Barton, Lien and Lunde developed the Q-system in 1974 and was last updated by Barton in 2002 (Barton , 2002). Rock quality index (Q) incorporates almost the same parameters as that of RMR system to assess the expected stability of the opening excavated in the rock mass. There is a parameter "Stress Reduction Factor (SRF)" in Q system which is different from RMR system and it involves the evaluation of in-situ stress state. The quality index (Q) values ranges from 0.001 to 1000 and it is calculated by using following expression:

$$Q = (RQD/Jn) \times (Jr/Ja) \times (Jw/SRF) \quad (3.3)$$

where

Jn = joint set number

Jr = joint roughness number

Ja = joint alteration number

Jw = joint water reduction factor

SRF = stress reduction factor

The geometry of the rock mass is represented by first quotient that is RQD/Jn. It represents the block or wedge size. Second quotient that is Jr/Ja represents the shear strength between the blocks. It reflects the joint's roughness and its frictional characteristics. Third quotient that is Jw/SRF represents the active stress state of the rock mass (Singh & Geol, 1999) (Hoek, 2007). Grimstad and Barton (1993) classified the rock mass as given in Table 3.3 based on Q values. Q value is used for the estimation of

- tunnel support requirements,
- length of rock bolt and maximum support spans,
- permanent pressure of roof support, and
- deformation modulus of the excellent quality rock mass

Table 3.3: Classification of rock mass according to Q-system (After Grimstad and Barton, 1993)

Rock Class	Q value	Rock Quality
A	400-1000	Exceptionally good
	100-400	Extremely good
	40-100	Very good
B	10-40	Good
C	4-10	Fair
D	1-4	Poor
E	0.1-1	Very poor
F	0.01-0.1	Extremely poor
G	0.001-0.01	Exceptionally poor

3.7.4 Geological Strength Index (GSI)

Hoek presented the GSI classification for the rock masses in 1994 to simplify the estimation of properties for competent and weak or fractured rocks for application in earth works (Hoek, 1994). It was developed by linking the conditions of the rock mass with experiences gained from the RMR-system (Singh and Geol, 1999). The relationship between the conditions of the rock mass and discontinuity is applied to determine an average value of GSI. It is suggested to use a range of GSI values instead of single value. GSI classification system is a fast, reliable and simple system. It can be used for computer simulation purposes as well to compute both the deformation and strength properties of a rock mass (Singh and Geol, 1999).

It is relatively a new classification scheme (Marinos, et al., 2006). It includes the diversity in geological materials resulting from the deformation and faulting of the rock mass. It provides reliable rock mass data required to use as input for closed form solutions or numerical analysis to design underground openings (Godwin, 2017). The GSI system was basically developed to estimate the Hoek-Brown strength parameters, deformability and rock mass strength. GSI system has some limitation as it considers the rock mass as an isotropic material (Singh and Geol, 1999).

3.7.5 Rock Mass Index (RMi)

Palmstrom proposed Rock Mass Index in 1995 to classify the strength of the rock mass. It represents the decrease in intrinsic strength of the rock mass because of the adverse effects of different joints (Singh and Geol, 1999) and it is stated as:

$$RMi = \sigma c \times Jp \qquad (3.4)$$

σc represents the uniaxial compressive strength and Jp describes jointing parameter of the rock mass. Jp incorporates four different joint characteristics that is joint roughness, joint density, joint alteration and joint size. Jp represents the effects of joints on the rock mass strength. Jp is given a value of 1 if the rock mass is intact and 0 if the rock mass is crushed (Singh and Geol, 1999). Palmstrom categorized the rock masses into different classes as shown in Table 3.4 based on RMi values.

Table 3.4: Rock mass characterization according to RMi (After Palmstorm, 1995)

RMi value	**Rock Mass Quality**
Less than 0.001	Extremely weak
0.001-0.01	Very weak
0.01-0.1	Weak
0.1-1	Medium
1-10	Strong
10-100	Very strong
More than 100	Extremely strong

During the feasibility studies of a project, RMi can be easily applied for the rough estimation of rock mass parameters (Palmstorm, 1995). Values of the Hoek-Brown Criterion parameter (s) can be simply and more precisely calculated using RMi, by the relationship $s = Jp^2$. Thus, the inputs of other classification systems can be improved by using RMi parameters.

3.7.6 Rock Mass Number (N)

Rock Mass Number (N) is the Q value of the rock mass when SRF is considered as 1 (Geol et al., 1995). The expression to estimate the value of N is given as under:

$$\text{Rock mass number (N)} = (RQD/Jn)(Jr/Ja)(Jw) \qquad (3.5)$$

Major rock mass classification systems are given in Table 3.5.

Table 3.5: Major rock mass classification systems for underground design (After Sepehri, 2016)

Rock Mass Classification System	Originator	Application and description
Terzaghi's rock mass classification	Terzaghi, 1946	Design of tunnel support based on the descriptive rock mass classification (that is intact rock, stratified rock, moderately jointed rock, blocky / seamy rock, crushed rock, squeezing rock and swelling rock)
Lauffer classification	Lauffer, 1958	Introduced the concept of stand-up time into the design of tunnel support. This concept is important because as the span increases, the time to install support decreases.
Rock quality designation (RQD) index	Deere et al., 1967	Estimation of rock mass quality from core logs, one of the key input data required to assess RMR, and Q. (details in section 3.7.1)
Rock structure rating (RSR)	Wichham et al., 1972	Design of the support, based on the concept of rating the important parameters: parameter A (geology), Parameter B (geometry) and Parameter C (groundwater and joint conditions). Consequently, RSR = A+B+C. Wichham et al. (1972) developed a design chart which the support parameters (such as shotcrete thickness, rock bolt spacing, steel rib spacing) can be estimated based on the RSR number.
Rock mass rating (RMR) system	Bieniawski, 1973	Design of underground structures (details in section 3.7.2)
Rock tunneling quality index (Q)	Barton et al., 1974	Design of support for underground structures (details in section 3.7.3)
Geological strength index (GSI)	Hoek, 1994	A key parameter to assess the Hoek-Brown failure criterion parameters. The lowest value of GSI is 10 for very poor rock masses and the maximum value of GSI is 100 for intact rock. (details in section 3.7.4)

3.8 Rock mass characterization of Potential hydro-electric project site

The major rock type encountered in tunnel construction is massive sandstone which is grey in color, medium grained, moderately fractured and sheared on right wall, thick to medium bedded and medium jointed having good to fair discontinuity surfaces with Calcite filling and an RQD value of 85 %. The rock is competent with favorable stress conditions and uniaxial compressive strength of 80 ± 10 MPa.

There are 2 dominant joint sets. The parameters of these joint sets are given as under:

1- Bedding joints have dip/dip direction in range 75-85/030-050. Spacing is 0.8-1.0m. These joints extend all along the tunnel span and no visible sign of termination (continues joints). Mostly planar/rough with infilling of non-swelling silty clay and calcite. Aperture varies from 2-5 mm.
2- Joint set (J1) have dip/dip direction in range 15-30/105-115. Spacing is 0.4-0.5m, persistence about 4-5m, mostly terminate into the bedding joints. Mostly planar/smooth with infilling of non-swelling silty clay and calcite. Aperture varies from 1-2mm.

In the tunnel areas under deep cover (potential rock burst damage areas), the rock mass is generally dry and large inflows or groundwater pressures have not been encountered. Minor seepage was observed; however, this is not considered sufficient to impact rock burst behavior.

3.8.1 Quality Index (Q) of rock mass

For the conditions given above the numeric values for the input parameters of Q system are given as under:

- RQD = 85 %
- Jn = 4
- Ja = 3
- Jr = 2
- Jw = 1
- SRF = 1

$$Q = (85/4) \times (2/3) \times (1/1) = 14$$

This value of Q indicates that the rock mass quality is good and belongs to "class B" that is Q_2. The equivalent dimension of the tunnel is given by following equation:

$$De = \frac{\text{Excavation span,diameter or height (m)}}{\text{Excavation Support Ratio (ESR)}} \qquad (3.6)$$

Diameter of the tunnel is 8 m and ESR for a hydro-power tunnel is 1.6. So,

$$De = 8/1.6$$

$$De = 5$$

This value of De suggests that the tunnel requires spot bolting. The bolt length is given by:

$$L = 2 + \frac{0.15\ B}{ESR} \quad (3.7)$$

$$L = 2 + \frac{0.15\ (8)}{1.6}$$

$$L = 8 \text{ m}$$

The maximum unsupported span is given by:

$$\text{Maximum span (unsupported)} = 2ESR\ Q^{0.4} \quad (3.8)$$

$$\text{Maximum span (unsupported)} = 9.2 \text{ m}$$

3.8.2 RMR of the rock mass

For the given rock mass conditions, the RMR value of the rock mass is computed as under:

$$RMR = 7+17+15+16+15 = 70$$

The RMR value also indicates that the rock mass quality is good and it belongs to class II. An RMR value of 70 suggests that the tunnel could be excavated by full face excavation with 1-1.5 m advance of face. Support should be completed at a maximum distance of 20 m from the face. Locally, rock bolts of 3 m length spaced at 2.5 m with occasional wire mesh is recommended for support. 50 mm of shotcrete is recommended in crown where required with no steel sets.

3.9 Summary

It is derived from above discussion that classification systems are intended to assist geologists and engineers to estimate the rock conditions where it is difficult to collect samples for testing or make field observations. Even though these systems provide a sound and measured estimate of rock conditions and aid communication at site still these systems can be improved further depending upon the further case histories.

The RMR rock mass classification is applied to cross check the quality of the rock mass proposed by the Q system. It is apparent from the Q and RMR values that the rock mass has good quality and less support requirements. The integration of rock reflects the capability of

rock to store energy, so it can also be used to reflect the rockburst tendency (Cai, 2016). So the larger the RQD/RMR/Q value, the more integrated the rock and the stronger the rockburst tendency. In our case, the good quality of rock has tendency to experience strong rock burst.

It should be noted that the rock mass quality varies along the different sections of the tunnel. However, this characterization is provided for the major rock type in which most of the excavation work is being carried out and rock burst phenomenon is observed in the same rock type.

Chapter 4 NUMERICAL MODELING

4.1 Introduction

In the recent past, numerical methods have become very popular due to rapid advancements in computer technology. The suitability of these methods for analysis and design of complex geotechnical problems is another reason for the popularity. Many conventional methods in rock mechanics are applicable to similar situations for which they were developed. However, there are many problems for which no experience is available. In such cases, numerical methods are the best option to solve the design problems. Moreover, numerical methods should be used as a complementary method along with analytical and empirical methods.

According to Sepehri (2016), numerical methods in rock mechanics can be classified into continuum, discontinuum and hybrid methods as described below:

Continuum methods are:

- The finite element method (FEM)
- The finite difference method (FDM)
- The boundary element method (BEM)

Discontinuum methods are:

- Discrete (or Distinct) elements method (DEM)
- Discrete fracture network (DFN)

Hybrid methods are:

- Hybrid FEM/BEM
- Hybrid DEM/BEM
- Hybrid FEM/DEM

The choice of continuum or discontinuum methods depends on the problem scale and the fracture system geometry. For example, if the displacement field is continuous and the medium has no discontinuities; thus, continuum numerical methods would be appropriate. Discontinuum methods are suitable for moderately fractured rock masses where large-scale displacements of individual blocks are possible (Jing, 2003). For example, if the

displacement is determined by a slip along the discontinuities and rotation of the blocks; in this case, discontinuum methods would be appropriate.

There is no absolute guide on which method is better than another and when one or another should be used. However, the disadvantages of each type can be avoided by using hybrid methods. For example, if the displacement field would be continuous inside each area; however, it may be discontinuous across the areas, so in this case, hybrid methods would be an appropriate choice (Bobet, et al., 2009).

FEM is a well-recognized numerical method which can be used for rock mechanics and geomechanical design problems. It can deal with material heterogeneity, anisotropy, non-linearity, complex boundary conditions, in-situ stresses and gravity (Jing and Hudson, 2002). For these reasons, in this research, FEM will be used as the main numerical method to perform the numerical analysis.

4.2 Finite Element Method (FEM)

FEM originated in early 1960s as an alternate to FDM to encounter the stress concentration problems in continuous materials to provide the numerical solutions of these problems. It was the first method for numerical solution of heterogeneous, non-linear and complex materials. FEM rapidly gained acceptance and became most widely used numerical method to solve problems in rock engineering. Another reason for its acceptance was the limitation of FDM to regular grids only by that time. Wide spread application of FEM started in late 1970s when many problems of rock mechanics were solved using FEM. FEM has been developing since then and today, still, it is the most widely applied method for numerical simulations of geo-mechanics (Nikolić, et al., 2016).

FEM is a numerical method to find the approximate solutions of boundary value problems related to differential equations. Generally, it divides the problem into smaller domains termed as finite elements, approximates locally for each element, assembles the finite elements and provides the solution for global matrix equation. FEM is a special case derivative of the Galerkin method to present the trial function globally, as compared to local approximation in FDM. A major advantage of FEM is the option to represent heterogeneous rocks that allows assigning varying material properties to the model. Infinite elements were also generated to simulate the effect of far-field in geotechnical projects (Nikolić, et al., 2016).

Usual FEM has some limitations as well to apply it efficiently in failure analysis, disturbance induce discontinuities and cracking because of the continuum assumptions. As the rock is discontinuous in nature while the FEM is continuum method, many attempts have been made to improve the method so that it can simulate the discontinuous effects and fracture propagation in rock mass (Ibrahimbegovic, 2009). Early investigations on rock samples showed that the stress-strain plots are non-linear up to rock failure. An early model "smeared-crack model" approximately simulated the non-linear behavior of stress-strain curve because of the crack opening. However, these smeared-crack models were completely brittle in its initial stages even though the rock has some inherent load-carrying ability after achieving its strength that results from the softening behavior of the rock (De Borst, et al., 2004).

During a structure collapse due to the progressive failure of the structural elements, the computation of ultimate load has been a key research topic for many researchers since it is very crucial failure mechanism. The main difficulty in such type of failure analysis is to correctly and mesh-independently represent the post-peak observed softening behavior during crack propagation. It is also critical to have very small sized elements and continuous re-meshing during crack propagation when simulating fracture growth using FEM. The 'enhanced' FE methods have been developing to beat these challenges and several new techniques inferred to help ease deficiencies of Standard FEM. ED-FEM (FEM with embedded discontinuities) can simulate fractures in each finite element, while X-FEM (Extended FEM) can represent the cracks globally (Fries and Belytschko, 2010; Armero and Kim, 2012; Dujc, et al., 2013). The X-FEM and ED-FEM strategies are comparable in their capacities to deal with the most challenging kinematics including both weak and strong discontinuities. Crack propagation is simulated along strong discontinuities, while weak discontinuities help to represent the material heterogeneous within each element. Additional discontinuous functions are added to standard kinematics of FEM that simulates the discontinuous behavior. Most recently, Nikolic et al. (2015) and Saksala, et al. (2015), contributed to ED-FEM technique in rock mechanics and simulated successfully the complex failures occurring in rocks.

Another enhanced FEM technique is G-FEM (Generalized FEM). The G-FEM applies local functions to the specific problems which are mostly analytical solutions. The benefit of G-FEM lies in its ability to represent the complex geometries easily because it generates mesh independent of the problem geometry. Additional functions and nodes are incorporated to

simulate the fractures. Another advantage of this technique is its ability to represent cavities which is vital for rock engineering purposes (Nikolić, et al., 2016).

FEM is not only suitable to represent heterogeneous materials but also it is an appropriate technique to represent inelastic and non-linear behaviors. It is also helpful to represent contact mechanisms, symmetrical non-linearities, fluid-structure interface, linking the scales from small scale (nano and micro) to large macro scales, etc. Enhanced FEM techniques make this method significantly more appealing on account of its abilities to simulate fractures without re-meshing. There are various commercial software available for finite element modeling of problems in rock engineering e.g. Phase^2, Plaxis, Flac3D, UDEC etc.

4.3 Application of FEM in rock burst analysis

The finite element method is suitable for the analysis of complex rock engineering problems such as rock burst (Sharan, 2007). However, little work has been done on the application of the finite element method for the instability analysis of rock burst. Bardet (1989) used the finite element method to analyze rock burst as a surface buckling problem. The computational technique was based on the eigen value approach. However, he assumed the rock mass to be hypo-elastic and applied the technique to the wedge-test problem.

In the application of the finite element method to problems in geomechanics, a computational difficulty arises due to the infinitely substantial extent of the geomaterial. Mitri, et al. (1999) used the finite element numerical modeling technique for the development of rock burst potential index in Canadian underground mines. Jin-shan, et al. (2007) used RFPA2D program for numerical modeling of rock burst and studied its effect in circular tunnels. Sharan (2007) used Phase^2 software for the finite element numerical modeling of the rock burst. Liu, et al. (2011) used Phase^2 software for the finite element numerical modeling and determination of the influential factors of the rock burst in a tunnel. Jarufe and Vasquez (2014) used Map3D and Unwedge software packages for numerical modeling of rock burst loading and to calculate the yielding support of a deep mine project. Sweby, et al. (2014) examined the numerical tools available to engineers, the scenarios in which they are applicable and the critical input parameters required for meaningful analysis in underground construction and used Phase^2 numerical modeling software for this purpose. Yi, et al. (2016) used numerical for both the forward planning and the back-analysis of simulated rock burst experiments.

4.4 RS^2 ($Phase^2$ 9.0) Software

According to Rocscience Inc., RS^2 (An updated version of Phase2) is a proficient 2-dimensional program for finite element analysis of rocks and soils (R=Rock, S=Soil, 2=2D). RS^2 can be utilized for an extensive variety of designing ventures and incorporates excavation design, probabilistic analysis, slope stability, consolidation, groundwater seepage, and dynamic investigation capabilities. Intricate, multi-stage design models can be effortlessly created and immediately analyzed e.g. tunnels in hard, competent, jointed or weak rocks, underground chambers for powerhouses, open pit mines, embankments, slopes, and many more. It can solve progressive and dynamic failure, support interface and many other earth related design problems.

A variety of modeling options are available for support installation and interaction. RS^2 offers to apply liner elements during the modeling of concrete, shotcrete, retaining walls, steel set systems, piles, geotextiles, multi-layer composite liners, etc. Support capacity can be plotted using a liner design option which allows the determination of safety factor for strengthened liners. Several types of bolts are included in RS^2 e.g. end anchored, split sets, fully bonded, grouted tiebacks and cable bolts.

An important feature of RS^2 is the use of reduction in shear strength method to analyze slope stability problems. It is a fully automated option and may be applied using either Hoek-Brown or Mohr-Coulomb strength parameters. It has an easy import or export option between SLIDE to easily compare finite element and limit equilibrium results for slope models.

RS^2 incorporates a built-in option for finite element analysis of groundwater seepage problem in steady state. There is no compelling reason to utilize a different groundwater program. Pore pressure, gradient and groundwater flow can be determined by defining material conductivity hydraulic boundary conditions. The results of pore pressure are automatically combined with stress analysis.

Mohr-Coulomb and Generalized Hoek-Brown material models can be created for varying rock and soil conditions. New features are added that enable the user to model jointed rock and automatically create discrete fracture or joint networks for a range of statistical models. With new 64-bit and multi-core equivalent processing systems, larger and further composite models can be solved using RS^2 in shorter times.

4.5 FE numerical Modeling of Potential Project using RS^2

In this section, a potential hydro-electric project site of parallel tunnels in Northern areas of Pakistan is used to implement the proposed research methodology. A full realistic two-dimensional (2D) elasto-plastic finite element model of the tunnels was developed. This finite element (FE) analysis model was used to determine the mining-induced stress regime at the tunnels. The results of the laboratory and in-situ tests conducted by tunnel construction companies were used to estimate the rock mass properties and calibrate the modeling input parameters used for the FE analysis.

The goal is to seek a detailed understanding of stress distribution regimes around the tunnels as a function of varying overburden depth and center to center distance between the tunnels. The results of the developed FE model are presented in chapters 5 for predictions and assessment of possible rock bursts in the tunnels.

4.5.1 Potential hydro-electric project site description

As far as past projects are concerned, sandstone of Murree formation caused major rock burst issues. The formation is located in the Muzaffarabad district of Azad Jammu Kashmir (AJK), Pakistan, northeast of Islamabad, near the existing Tarbela and Mangla hydroelectric projects. The project includes a 160-m-long, 56-m-high concrete gravity and rockfill diversion dam on the Neelum River. The dam will create a head pond of about ten million m^3, which will allow a peaking reservoir of 3.80 million m^3 to meet daily peaking of power for about four hours. A six-gated intake structure of 280 m^3/sec capacity will be connected through three conventional surface sedimentation basins to the headrace tunnel.

The project faced very challenging Himalayan geologic conditions including high rock cover (up to 1900 m), squeezing ground, and very high earthquake hazard. Construction, which started in 2008, involves more than 52 km of large diameter tunneling mostly by drill-and-blast. From intakes to tailrace, the headrace tunnel is 28.5 km in length with an average 11 m equivalent diameter in rock. A 19.6 km stretch of the tunnel from the Nauseri site will be constructed as a twin tunnel system, each with a cross section of about 52 m^2 with a center to center distance of 33 m; 11.2 km of the twin tunnel system will be excavated by Tunnel Boring Machines (TBM) and the remainder by drill-and-blast. The remaining headrace tunnel to the surge chamber will be a single tunnel having a cross section of 100 m^2.

The drill-and-blast tunnels will be concrete-lined and the TBM excavated tunnels will be shotcrete-lined with a concrete invert. The headrace tunnel crosses under the Jhelum River and passes through the seismically active Muzaffarabad fault. Construction of the underground works requires seven adits for access of resources and removal of excavated spoil. Construction of the project has required design and construction of more than 25 km of new roads and upgrading of about 175 km of existing roads and bridges.

The project is in rocks belonging to the Murree Formation except at the intake, which is partly in igno-metamorphic rocks belonging to the Panjal Formation. The latter group of rocks is located on the right side of the Neelum River. The parallel tunnels are designed for the Murree Formation. The Murree Formation at the location of the parallel tunnels consists of alternating beds of grey medium to fine grained sandstone and reddish colored fine to very fine gained siltstone with occasional thin mudstone layers. Contacts are often gradational with no bedding parting. Two sandstones, SS1 and SS2, siltstone and occasional thin mudstone beds are recognized. Thick SS1 sandstone beds are often very massive and competent. Bedding is normally steep dipping, striking roughly normal to the tunnel bearing. Folding and faulting can create locally anomalous structural conditions. Tunneling in SS1 initiated major rock bursts hence the focus of this study is SS1.

4.5.2 Rock mass properties

The behavior of the rock was assumed to be governed by an elastic-plastic constitutive relation based on the elasticity theory and the Mohr-Coulomb plasticity criterion. Based on site investigation, in-situ and laboratory testing the material properties used for the modeling are shown in Table 4.1.

Table 4.1: Material properties for potential hydro-electric project site

Lithology	UCS (MPa)	Poison's Ratio	Density (Kg/m^3)	Unit Weight (MN/m3)	Slake Durability %	Tensile Strength (MPa)	K (in-plane)	K (out of plane)
Sandstone	86	0.27	2705	0.026536	98.95	9.65	2.05	1.04

Mohr-Coulomb strength parameters for different rock covers are given in Table 4.2.

Table 4.2: Rock strength parameters for different rock covers

Rock mass	Parameters	200 m rock cover		500 m rock cover		800 m rock cover		1200 m rock cover		1500 m rock cover		1800 m rock cover	
		P	R	P	R	P	R	P	R	P	R	P	R
Sandstone	Cohesion (MPa)	2.0	1.3	3.0	2.2	3.9	2.8	4.9	3.6	5.6	4.1	6.2	4.6
	Friction Angle (Deg)	55.5	49.6	49.4	42.9	46.0	36.2	42.8	36.0	41.1	34.2	39.7	32.8
	Deformation Modulus (GPa)	20.2	7.3	20.2	7.3	20.2	7.3	20.2	7.3	20.2	7.3	20.2	7.3

(P=Peak, R=Residual)

4.5.3 Software parameters for analysis

Following software parameters were used for the analysis of stresses around the tunnels under different overburden:

- Number of stages were selected as 3 initially to analyze the excavation of tunnels one by one. Later it was reduced to 2 to analyze the simultaneous excavation of tunnels.
- Plain strain analysis type was used with Gaussian Elimination.
- Two parallel tunnels were drawn with a diameter of 8.14 m each and a center to center distance of 33 m. Later the center to distance was varied to analyze the effect of pillar width on stress redistribution.
- A graded mesh type with 3 noded triangles and a gradation factor of 0.1 was used for meshing and discretization purpose.
- A gravity type field stress was applied to analyze the effect of different rock covers on stress regime and XY restraints were applied on boundary.
- Material properties are used as given in Table 4.1 and Table 4.2.

4.5.4 Model for Overburden analysis

Initially, the models were run as a separate excavation of tunnels that is first excavated a tunnel in a stage and then excavated the other tunnel in next stage. To analyze the effect of overburden on rock burst occurrence in tunnels, different models are analyzed for overburden thickness of 200 m, 500 m, 800 m, 1200 m, 1500 m and 1800 m. An example of the model for 200 m overburden thickness is shown in Figure 4.1.

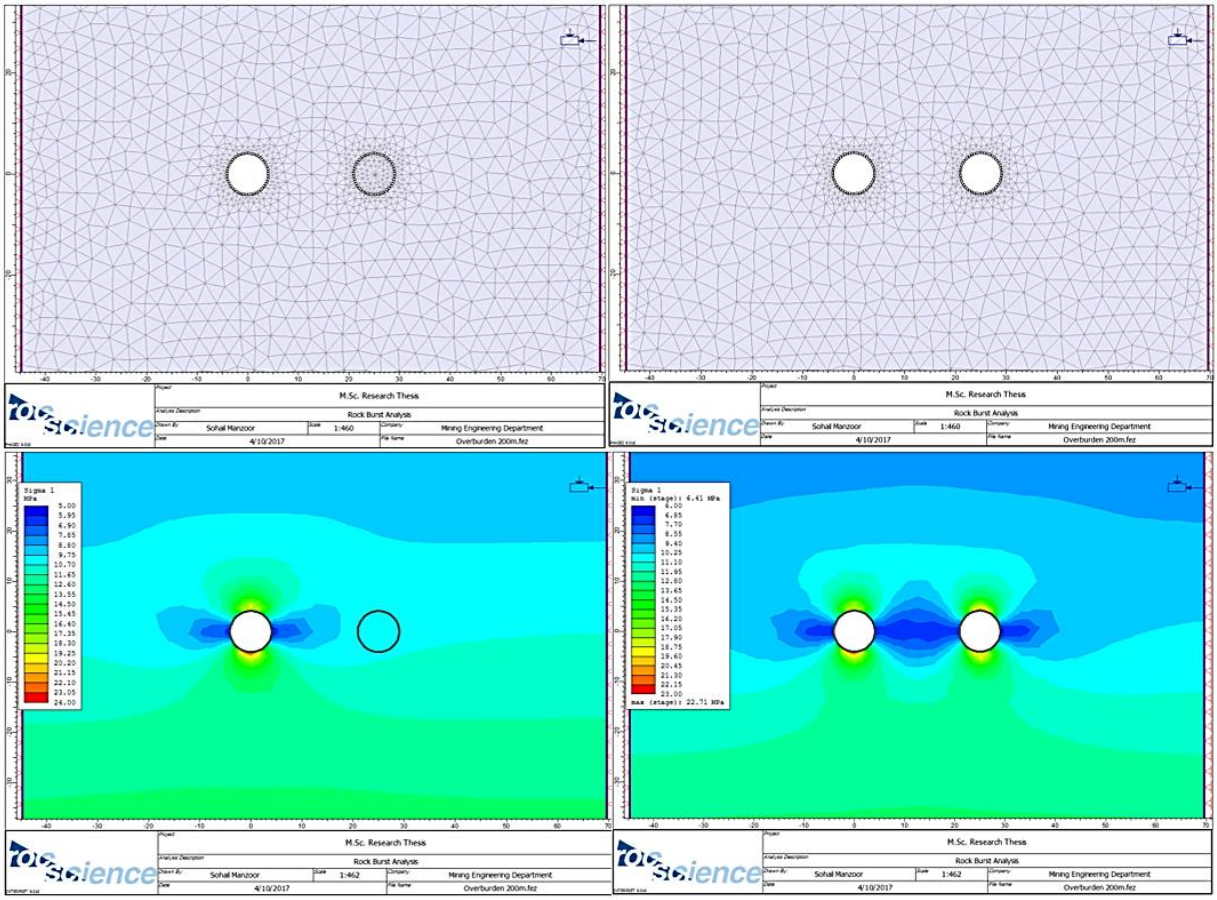

Figure 4.1: RS2 Model to analyze the stress redistribution at a depth of 200 m for sequential excavation of tunnels

The figure shows that the maximum tangential stress is acting at the crown and invert of the tunnels. The walls and the pillar between the tunnels are safe. So, the maximum values of these stresses are assessed using tangential stress criterion for rock burst assessment in Chapter 5.

4.5.5 Model for excavation sequence analysis

After the analysis of overburden thickness on rock burst occurrence with tunnel excavation in 2 distinct stages, analysis is run for simultaneous excavation of both tunnels. Models are analyzed for overburden thickness of 200 m, 500 m, 800 m, 1200 m, 1500 m and 1800 m. An example of the model for 200 m overburden thickness with simultaneous excavation of both tunnels is shown in Figure 4.2.

Figure 4.2 shows a similar trend in stress redistribution as was observed in Figure 4.1. However, it is observed that there is slight decrease in maximum tangential acting on the tunnel when both tunnels are excavated simultaneously. That is probably due to the mutual impact of the tunnels on each other. Rock burst assessment for these stresses is carried out in Chapter 5.

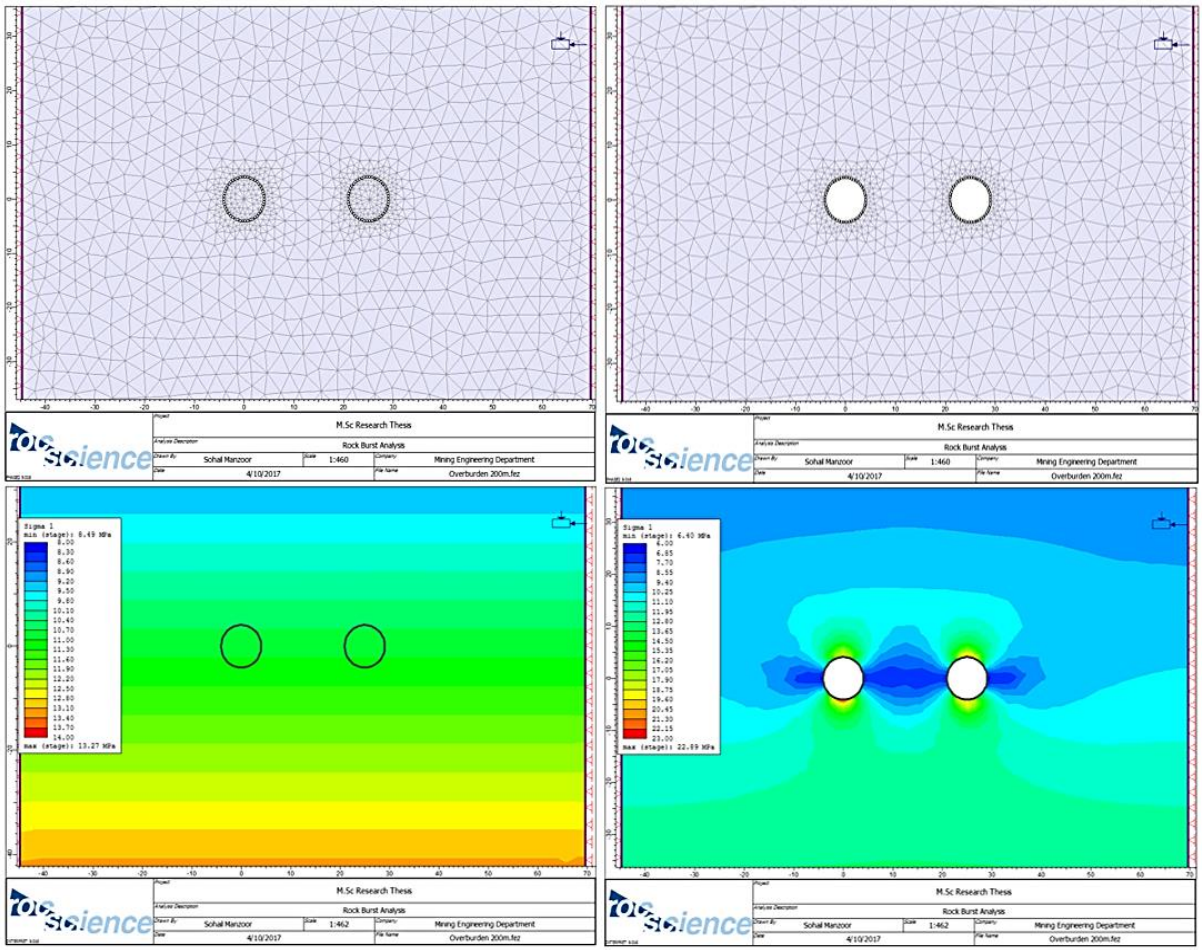

Figure 4.2: RS2 Model to analyze the stress redistribution at a depth of 200 m with simultaneous excavation of parallel tunnels

4.5.6 Model for pillar width analysis

To analyze the effect of pillar width on stress redistribution and to select an optimum pillar width, different models are run for pillar widths of 15 m, 20 m, 25 m, 30 m, 35 m, 40 m, 45 m, 50 m, 55 m, 60 m, 65 m and 70 m. These models are run for both conditions discussed in sections 4.5.4 and 4.5.5 that is sequential excavation of tunnels and simultaneous excavation of tunnels. The result of this analysis is discussed in chapter 5.

4.5.7 Model for support analysis

To analyze the effect of different supports and select an optimum support for the project, different models are run for an optimum pillar width of 25 m under a maximum rock cover of 1800 m with the elasto-plastic conditions of the rock mass. Yielded elements and total displacement of tunnels for different support conditions are shown in Figures 5.18 to 5.25 with respective interpretation of results.

4.6 Summary

Numerical modelling is a useful tool in simulation of problems encountered in rock mechanics. In this chapter, a review of finite element numerical modelling in rock mechanics is presented. The main objective was to develop an integrated engineering methodology to estimate mining-induced stress regimes in the host rock using the FE analysis method. The methodology utilized the commercially available FE software called RS^2.

Numerical models were developed to analyze the effect of varying overburden thickness, excavation sequence and pillar width between the parallel tunnels on the mining-induced stress regime around the tunnel. At the end, support requirements for the tunnels were analyzed by developing FE models for the installation of different rock bolts and liners in the tunnels.

Chapter 5 ROCK BURST ASSESMENT

5.1 Introduction

Rock burst is an instantaneous and violent failure of rock which occurs when a volume of rock is strained beyond its elastic limit. According to the Mine Safety and Health Administration, a rock burst can be defined as "a sudden and violent failure of a large volume of overstressed rock, resulting in the instantaneous release of substantial amounts of accumulated energy" (Sepehri, 2016).

Numerical methods are frequently used to solve the problems encountered in intricate underground excavation activities. These methods provide researchers and engineer the most suitable tool to recognize and evaluate the failure mechanisms and predict the geotechnical risks associated with any underground excavation activity more effectively. In numerical modelling technique, when linear elastic models are used to analyze any underground opening, it doesn't offer full interpretation of the true stress state. Therefore, elasto-plastic models of the material are used to eliminate the inadequacy of linear elastic models. Hence, predicting likelihood of failure by finite element (FE) numerical modeling becomes essential (Abdellah, 2013).

In this chapter, rock burst occurrence is predicted using the developed finite element analysis models and analytical approach of tangential stress criterion for rock burst assessment. In the end, recommendations are formulated to minimize the likelihood of rock burst in tunnels and suggestions are made for future work.

5.2 Tangential stress Criterion for rock burst assessment

This method considers the strength property of the rock and induced tangential stress (environmental factor) in the rock mass. Therefore, both conditions required for a rock burst to occur can be evaluated. The tangential stress (Ts) criterion can be estimated using equation below:

$$T_S = \sigma_\theta / \sigma_c \tag{5.1}$$

where, σ_c is the UCS of the rock and σ_θ is the tangential stress around the underground opening (that is stopes, drifts, etc.). According to Wang and Park (2001), the rock burst tendency can be evaluated using Ts criterion as presented in table 5.1.

Table 5.1: Rock burst assessment using the tangential stress criterion (After Wang and Park, 2001)

Tangential Stress Criterion (Ts)	Rock burst tendency
Ts < 0.3	No rock burst
0.3 ≤ Ts < 0.5	Weak
0.5 ≤ Ts < 0.7	Strong
Ts ≥ 0.7	Violent

5.3 Rock burst assessment for potential hydro-electric project site

In following sections, the results of FE models are assessed using tangential stress criterion to predict the tendency of rock burst occurrence and potential areas susceptible for rock bust occurrence. Overburden thickness, excavation sequence and pillar width are analyzed to select a suitable excavation sequence and an optimum pillar width.

5.3.1 Overburden analysis

In this section, various FE models are computed to analyze the effect of overburden thickness on rock burst occurrence. Tunnels were in excavated in 2 different stages. The tunnel being excavated first was named as “Tunnel 1” and the one being excavated after that was named as “Tunnel 2” for our analysis purpose. Stress redistribution was analyzed for overburden thickness of 200 m, 500 m, 800 m, 1200 m, 1500 m and 1800 m. The procedure to apply the rock burst assessment criterion using the results of FE models is illustrated for a rock cover of 200 m. The assessment results for remaining rock covers are given in Table 5.2 to 5.5.

Stress redistribution at 200 m depth around Tunnel 1 is shown in Figure 5.1. The maximum tangential stress at the crown of the tunnel is 18.71 MPa which is concentrated 0.9 m away from the crown of the tunnel. The maximum tangential stress at the invert of the tunnel is 23.77 MPa acting at the boundary of the tunnel. Stress redistribution around Tunnel 2 is shown in Figure 5.2. The maximum tangential stress at the crown of the tunnel is 21.99 MPa acting at the boundary of the tunnel. The maximum tangential stress at the invert of the tunnel is 18.96 MPa which is concentrated 0.9 m away from the invert of the tunnel.

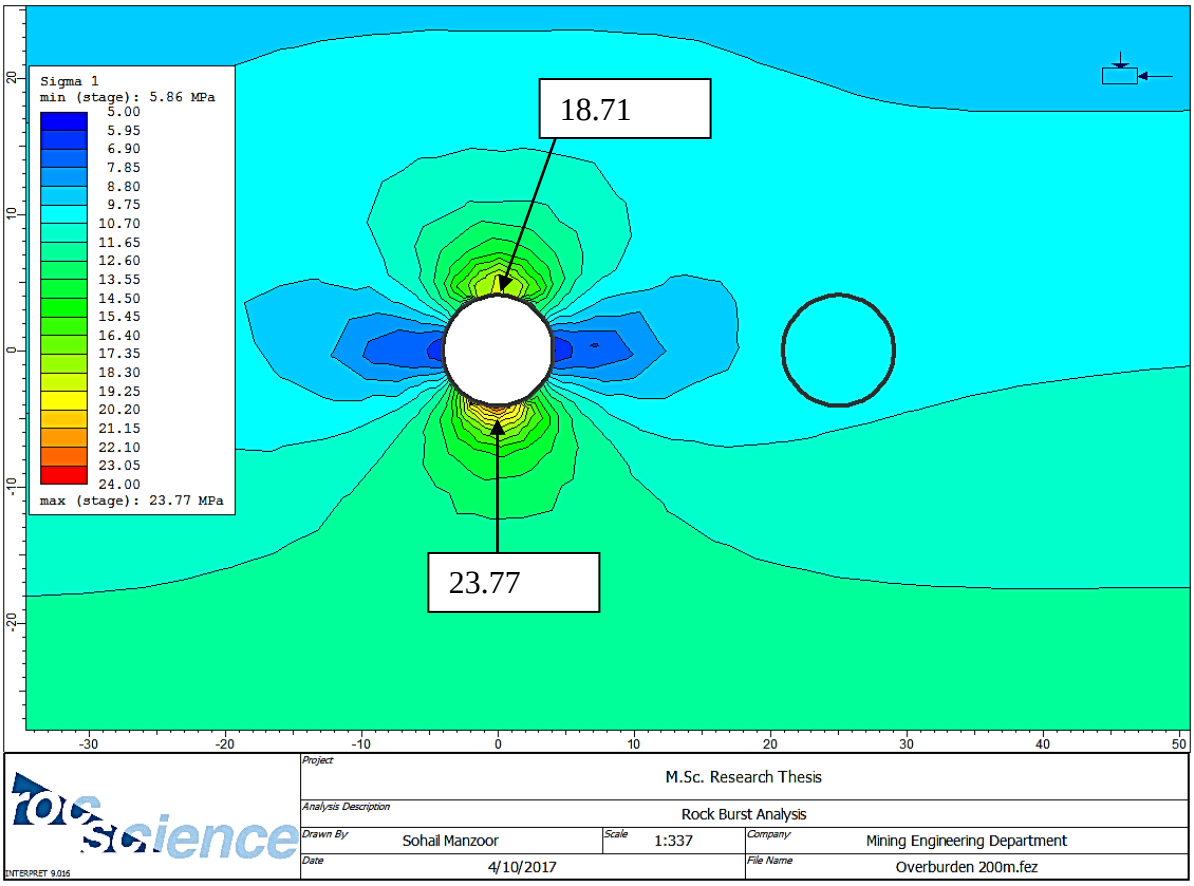

Figure 5.1: RS2 model showing the max. tangential stresses at the crown and invert of Tunnel 1 at 200 m depth

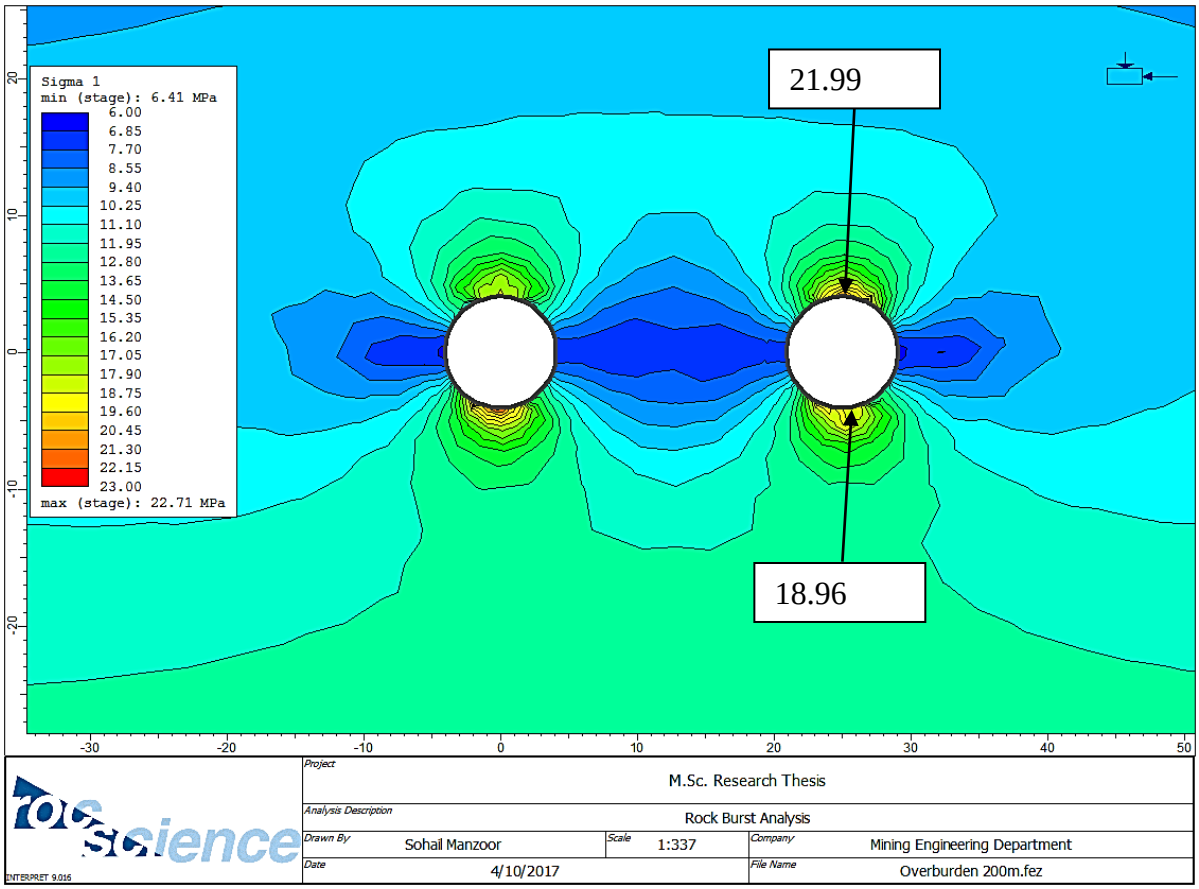

Figure 5.2: RS2 model showing the max. tangential stresses at the crown and invert of Tunnel 2 at 200 m depth

Using the tangential stress criterion, Ts at the crown of Tunnel 1 is determined as:

$$Ts = {}^{18.71}/_{86} = 0.22$$

Ts at the invert of Tunnel 1 is determined as:

$$Ts = {}^{23.77}/_{86} = 0.28$$

As the value of Ts is less than 0.3 for both sections of the tunnel, there is no tendency of rock burst occurrence in Tunnel 1. Similarly, Ts at the crown of Tunnel 2 is given as:

$$Ts = {}^{21.99}/_{86} = 0.26$$

And, Ts at the invert of Tunnel 2 is calculated as:

$$Ts = {}^{18.96}/_{86} = 0.22$$

As the value of Ts is less than 0.3 for both sections of the tunnel, there is no tendency of rock burst occurrence in Tunnel 2 as well at a depth of 200 m. Similarly, the both tunnels were analyzed at further depths and results are summarized in Table 5.2 to Table 5.5.

Table 5.2: Rock burst assessment at the crown of Tunnel 1 at various depths

Depth (m)	**σ_c (MPa)**	**σ_θ (MPa)**	**Distance of σ_θ from the crown (m)**	**Ts = σ_θ / σ_c**	**Rock burst tendency**
200	86	18.71	0.9	0.22	No
500	86	42.28	1.6	0.49	Weak
800	86	69.44	3.0	0.81	Violent
1200	86	94.32	3.6	1.10	Violent
1500	86	110.61	4.8	1.29	Violent
1800	86	135.44	5.7	1.57	Violent

Table 5.3: Rock burst assessment at the invert of Tunnel 1 at various depths

Depth (m)	**σ_c (MPa)**	**σ_θ (MPa)**	**Distance of σ_θ from the invert (m)**	**Ts = σ_θ / σ_c**	**Rock burst tendency**
200	86	23.77	0	0.28	No
500	86	43.88	1.7	0.51	Strong
800	86	69.69	2.9	0.81	Violent
1200	86	102.77	3.9	1.20	Violent
1500	86	113.11	5.5	1.32	Violent
1800	86	136.61	6.3	1.59	Violent

Table 5.4: Rock burst assessment at the crown of Tunnel 2 at various depths

Depth (m)	σ_c (MPa)	σ_θ (MPa)	Distance of σ_θ from the crown (m)	Ts = σ_θ / σ_c	Rock burst tendency
200	86	21.99	0	0.22	No
500	86	40.63	1.5	0.49	Weak
800	86	64.55	2.7	0.81	Violent
1200	86	91.07	3.5	1.10	Violent
1500	86	107.36	4.6	1.29	Violent
1800	86	128.21	5.7	1.57	Violent

Table 5.5: Rock burst assessment at the invert of Tunnel 2 at various depths

Depth (m)	σ_c (MPa)	σ_θ (MPa)	Distance of σ_θ from the invert (m)	Ts = σ_θ / σ_c	Rock burst tendency
200	86	18.96	1.1	0.28	No
500	86	40.85	2.1	0.51	Strong
800	86	64.37	2.9	0.81	Violent
1200	86	86.09	4.1	1.20	Violent
1500	86	109.77	4.8	1.32	Violent
1800	86	133.35	5.2	1.59	Violent

The distance of σ_θ from the crown or invert shows the location of concentration of maximum stresses which is the depth of failure. For example, a maximum stress of 133.35 MPa is acting at 5.0 m from the tunnel invert, it will break and move at least 5 m rock material below the tunnel invert, causing a rock burst failure depth of 5 m. The relationship between the overburden thickness and maximum tangential stress, depth of failure and rock burst tendency is shown in Figures 5.3-5.11.

5.3.1.1 Relationship between overburden thickness and σ_θ

The relationship between the overburden thickness and maximum tangential stress at the crown of Tunnel 1 is shown in Figure 5.3. The graph shows a linear relationship between the depth of tunnel and the tangential stresses that means with the increase in tunnel depth, there is a linear increase in tangential stresses. From this graph, we can find out the maximum tunnel depth up to which the tunnel crown is safe. According to the tangential stress criterion, there is no tendency of rock burst up to Ts < 0.3. So,

$$\sigma_\theta/\sigma_c = \sigma_\theta/86 = 0.3$$

$$\sigma_\theta = 0.3 \times 86 = 25.8 \text{ MPa}$$

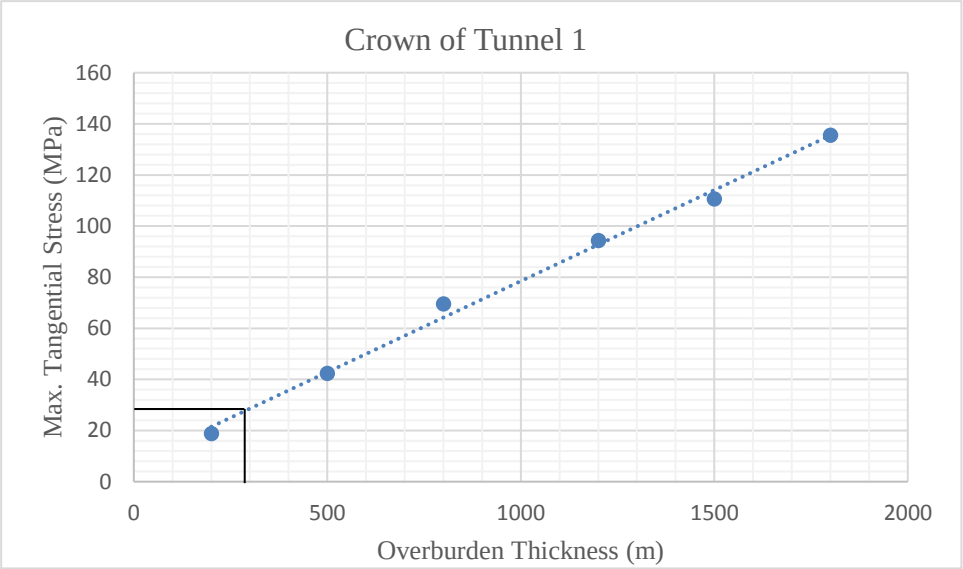

Figure 5.3: Relationship between the overburden thickness and max. tangential stress at the crown of Tunnel 1

So, the crown of the tunnel 1 is safe up to a tangential stress of 25.8 MPa that will be acting on the tunnel at a depth of 275 m (extracted from the graph shown in figure 5.3) after which it will be susceptible to rock burst occurrence.

The relationship between the overburden thickness and maximum tangential stress at the invert of Tunnel 1 is shown in Figure 5.4.

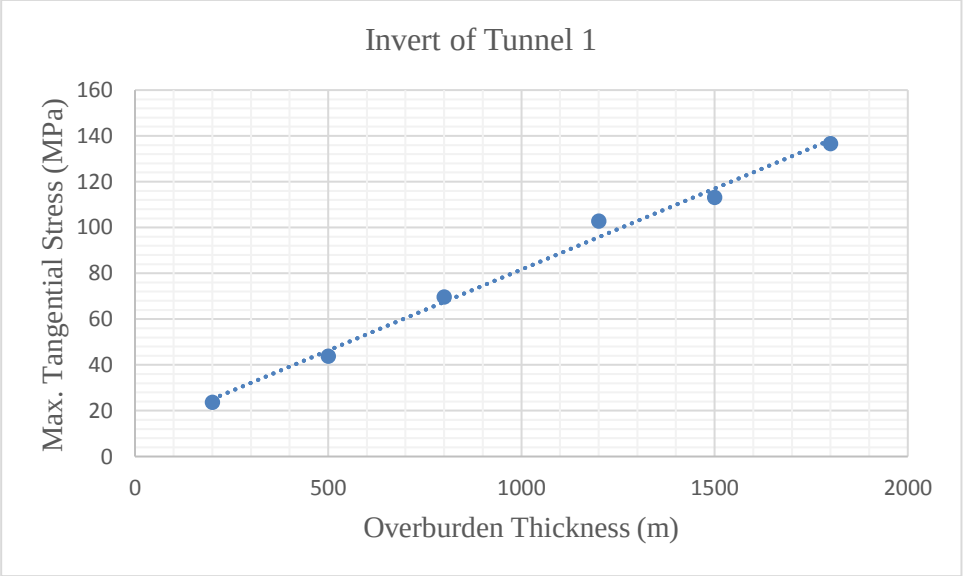

Figure 5.4: Relationship between the overburden thickness and max. tangential stress at the invert of Tunnel 1

Figure 5.4 shows the similar trend and hence we can calculate the safe depth of tunnel with respect to invert of the tunnel in the same way as we calculated for crown of the tunnel. From graph in Figure 5.4, the safe depth of tunnel for the invert of Tunnel 1 comes to be 230 m after which it will be prone to rock burst hazard.

A comparison of tangential stresses for the crown and invert of Tunnel 1 is made in Figure 5.5.

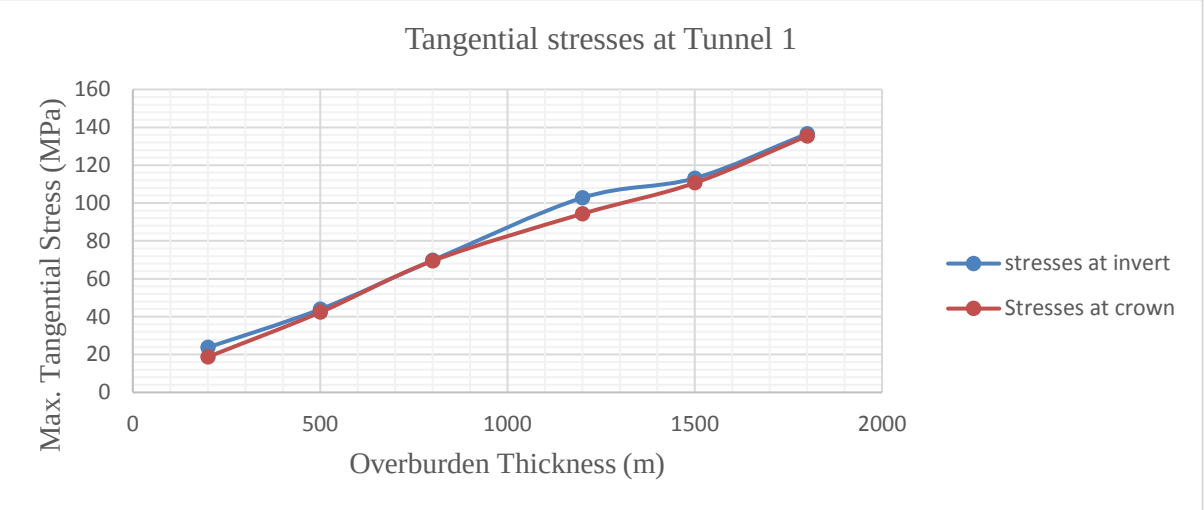

Figure 5.5: Comparison of stresses at crown and invert of Tunnel 1

Figure 5.5 shows that the stresses acting at the invert of the tunnel are slightly higher than the crown of the tunnel suggesting that there is slightly higher risk of rock burst event at the invert as compared to the crown of the tunnel.

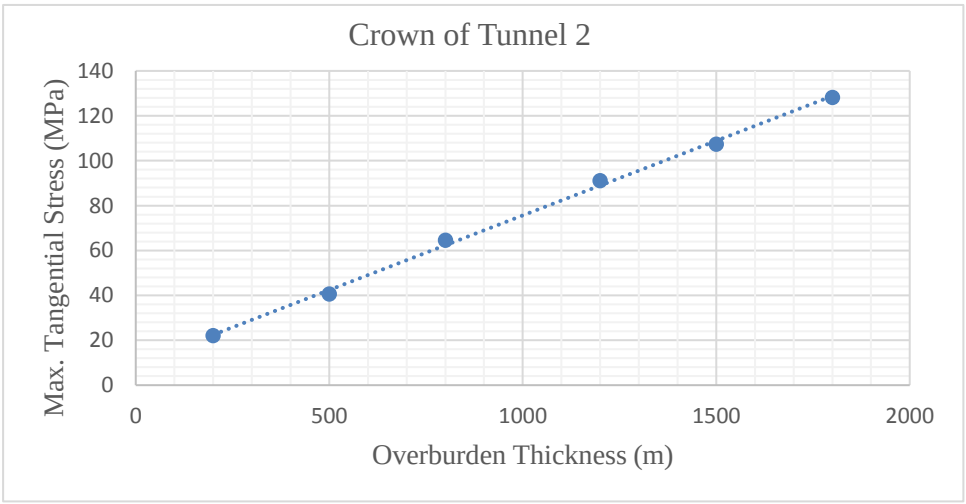

Figure 5.6: Relationship between the overburden thickness and max. tangential stress at the crown of Tunnel 2

The relationship between the tunnel depth and maximum tangential stresses at the crown and invert of Tunnel 2 are illustrated in Figure 5.6 and Figure 5.7 respectively.

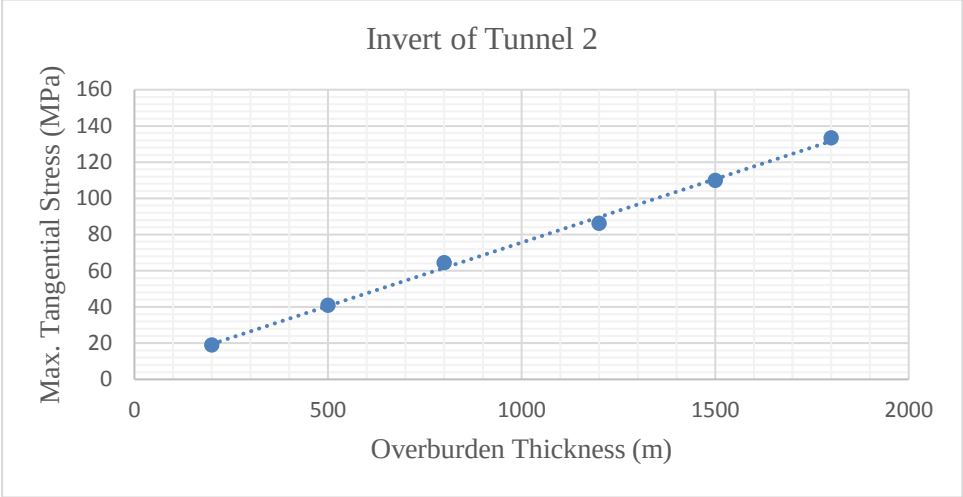

Figure 5.7: Relationship between the overburden thickness and max. tangential stress at the invert of Tunnel 2

Figures 5.6 and 5.7 shows similar trend as observed in Figures 5.3 and 5.4. Therefore, adopting the similar procedure the maximum safe depth of the tunnel 2 is calculated from Figure 5.6 and Figure 5.8. The crown of Tunnel 2 is safe up to a depth of 250 m and invert of the Tunnel 2 is safe up to a depth of 280 m after which it will be prone to rock burst hazard.

5.3.1.2 Relationship between overburden thickness and failure depth

The relationship between the tunnel depth and failure depth at the crown and invert of Tunnel 1 is shown in Figures 5.8 and Figure 5.9, respectively.

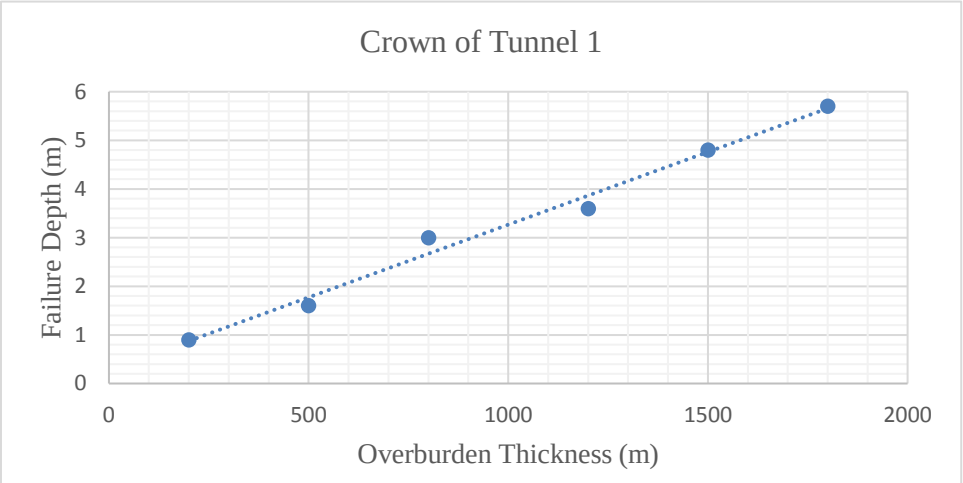

Figure 5.8: Relationship between overburden thickness and failure depth at crown of Tunnel 1

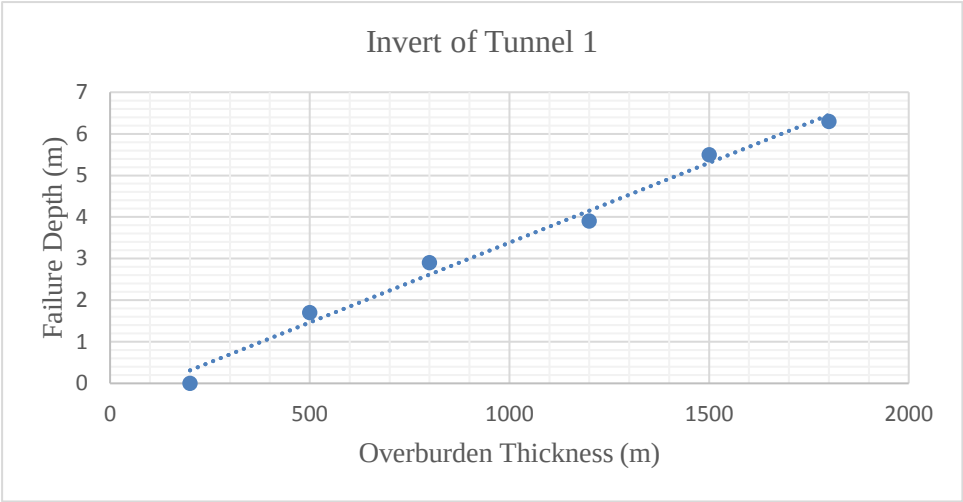

Figure 5.9: Relationship between overburden thickness and failure depth at invert of Tunnel 1

Figures 5.8 and 5.9 show a linear relationship between the tunnel depth and failure depth at the crown and invert of Tunnel 1 which indicates that with the increase in overburden thickness, the rock burst depth also increases linearly. The relationship of tunnel depth and failure depth for the Tunnel 2 are illustrated in Figures 5.10 and 5.11.

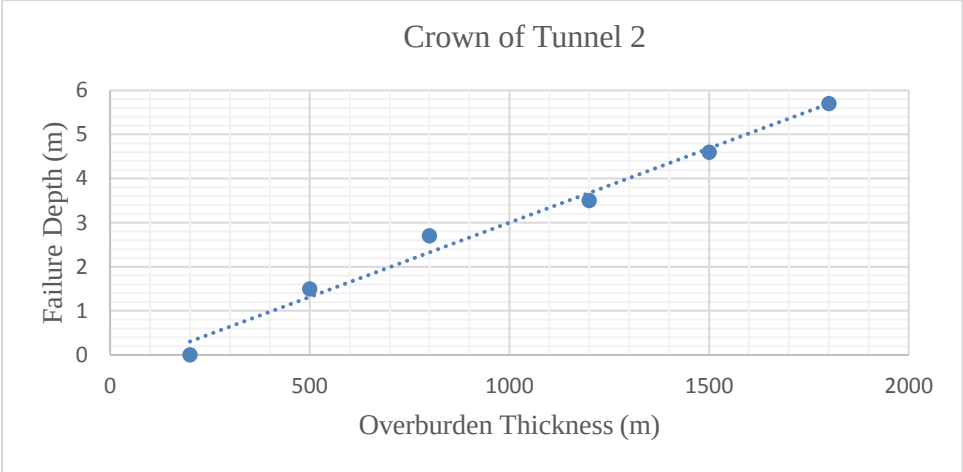

Figure 5.10: Relationship between overburden thickness and failure depth at crown of Tunnel 2

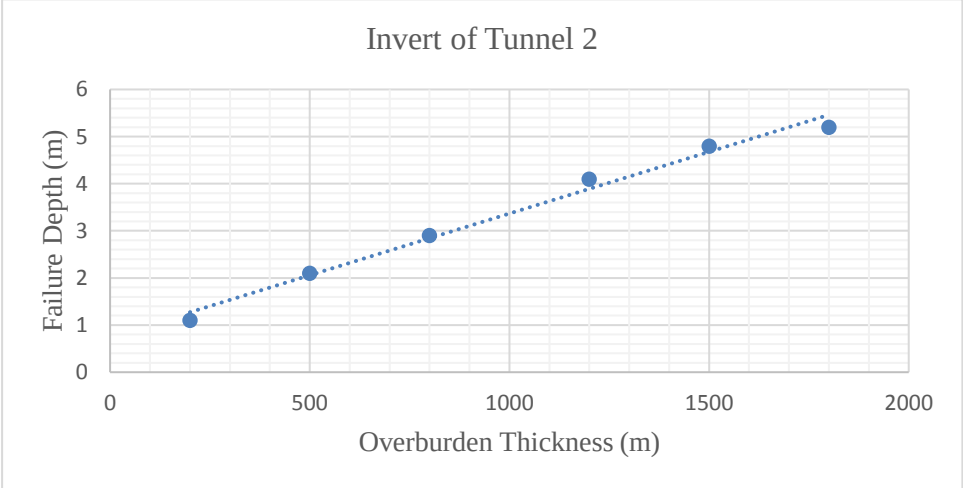

Figure 5.11: Relationship between overburden thickness and failure depth at invert of Tunnel 2

The relationships between the tunnel depth and rock burst failure depth tend to be linear as shown in Figures 5.8-5.11. Using these relationships, the rock burst depth at any tunnel depth can be approximated easily and quickly. The actual rock burst depth can vary from the predicted failure depths but it can be a useful tool to estimate the depth for destressing procedures etc.

5.3.2 Excavation sequence analysis (Elasto-Plastic Models)

During the overburden analysis of Tunnel 1, it was observed that the maximum tangential stress around the Tunnel 1 decreased when the second tunnel was excavated in next stage due to the mutual impact of tunnels. This observation led to the assumption that overall tangential stress acting on parallel tunnels will be relatively lower if excavated simultaneously than separate excavation of tunnels. In the following sub-sections, both the tunnels are excavated simultaneously to analyze the stress redistribution and their effect on rock burst occurrence and depth of failure. Stress redistribution was analyzed for overburden thickness of 200 m, 500 m, 800 m, 1200 m, 1500 m and 1800 m. The procedure to apply the rock burst assessment criterion using the results of FE models is the same as discussed in section 5.3.1. The assessment results are given in Table 5.6-5.9.

Table 5.6: Rock burst assessment at the crown of Tunnel 1 at various depths

Depth (m)	**σ_c (MPa)**	**σ_θ (MPa)**	**Distance of σ_θ from the crown (m)**	**Ts = σ_θ / σ_c**	**Rock burst tendency**
200	86	18.15	0	0.21	No
500	86	39.93	1.1	0.46	Weak
800	86	64.25	3.3	0.75	Violent
1200	86	92.01	3.3	1.07	Violent
1500	86	99.22	6.4	1.15	Violent
1800	86	123.45	3.9	1.44	Violent

Table 5.6 shows the stress values and rock burst tendency at crown of Tunnel 1 for varying overburden thickness when excavated simultaneously with tunnel 2. It slightly lower values of tangential stresses acting at the crown of the Tunnel 1 as compared to the values given in Table 5.2. This comparison validates the assumption that simultaneous excavation of the parallel tunnels lowers the tangential stresses acting at the tunnels. This comparison is further illustrated in Table 5.10 and Figure 5.12.

Table 5.7: Rock burst assessment at the invert of Tunnel 1 at various depths

Depth (m)	σ_c (MPa)	σ_θ (MPa)	Distance of σ_θ from the invert (m)	Ts = σ_θ / σ_c	Rock burst tendency
200	86	22.89	0	0.27	No
500	86	42.56	1.7	0.49	Weak
800	86	67.73	3.2	0.79	Violent
1200	86	96.84	3.4	1.13	Violent
1500	86	108.17	3.5	1.26	Violent
1800	86	129.13	4.3	1.50	Violent

Table 5.8: Rock burst assessment at the crown of Tunnel 2 at various depths

Depth (m)	σ_c (MPa)	σ_θ (MPa)	Distance of σ_θ from the crown (m)	Ts = σ_θ / σ_c	Rock burst tendency
200	86	21.98	0	0.26	No
500	86	39.74	1.3	0.46	Weak
800	86	64.55	3.3	0.75	Violent
1200	86	90.42	3.3	1.05	Violent
1500	86	110.21	3.7	1.28	Violent
1800	86	129.28	5.1	1.50	Violent

Table 5.9: Rock burst assessment at the invert of Tunnel 2 at various depths

Depth (m)	σ_c (MPa)	σ_θ (MPa)	Distance of σ_θ from the invert (m)	Ts = σ_θ / σ_c	Rock burst tendency
200	86	20.03	0	0.23	No
500	86	41.15	2.9	0.48	Weak
800	86	64.61	3.1	0.75	Violent
1200	86	86.51	4.3	1.01	Violent
1500	86	110.01	4.9	1.28	Violent
1800	86	135.05	5	1.57	Violent

Table 5.10: Comparison of maximum tangential stresses observed in sequential and simultaneous excavation of tunnels in Elasto-Plastic Models

Depth (m)	Maximum Tangential Stress with sequential excavation of tunnels (MPa)	Maximum Tangential Stress with simultaneous excavation of tunnels (MPa)
200	23.77	22.89
500	43.88	42.56
800	69.69	67.73
1200	102.77	96.84
1500	113.11	110.01
1800	136.61	135.05

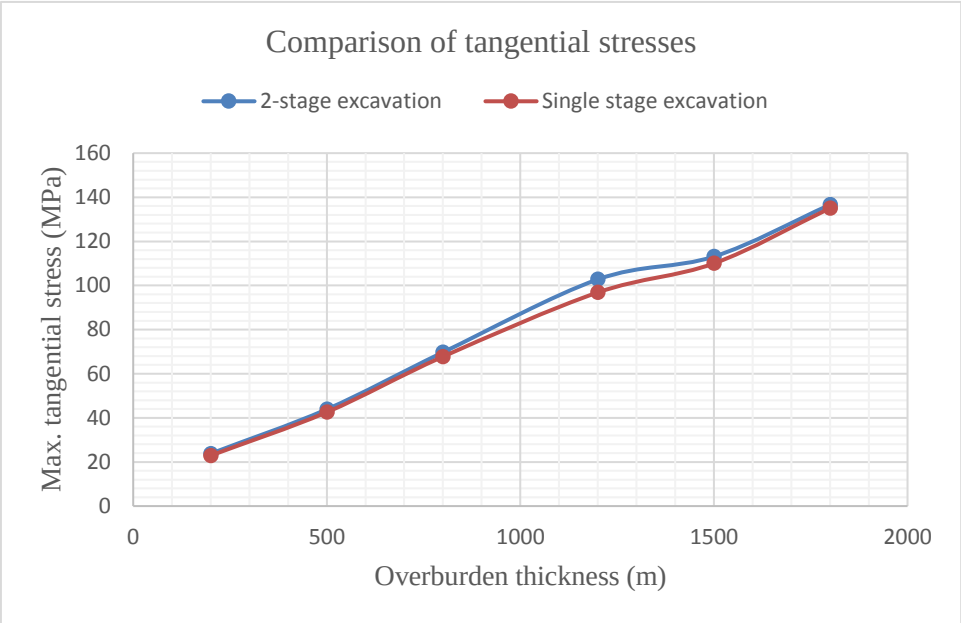

Figure 5.12: Comparison of tangential stresses for sequential and simultaneous excavation of tunnels

Figure 5.12 shows that there is a slight decrease in maximum tangential stress acting either on Tunnel 1 or Tunnel 2 when excavated simultaneously as compared to separate excavation of tunnels. However, this decrease is not significant enough to have an impact on rock burst occurrence. Therefore, the excavation sequence doesn't have much effect in decreasing the possibilities of rock burst occurrence.

5.3.3 Pillar width analysis (Elasto-Plastic Models)

The center to center distance between the tunnels was increased to 55 m after the rock burst event at the tunnel site. The maximum overburden for the tunnels is approximately 1800 m. So, at this depth, an optimum pillar width was determined by analyzing the maximum stresses for pillar widths of 15 m, 20 m, 25 m, 30 m, 35 m, 40 m, 45 m, 50 m, 55 m, 60 m, 65 m and 70 m. The observed maximum stress values for sequential and simultaneous excavation of tunnels at a depth of 1800 m are given in Table 5.11.

The relationship between the pillar width and the maximum stresses is illustrated in Figures 5.13 and 5.14. It is important to observe that the stress values change up to a pillar width after which there is almost negligible change in stresses suggesting that both tunnels affect each other up to that pillar width after which the tunnels start to behave independently without affecting each other.

Table 5.11: Maximum tangential stress acting on tunnels for different pillar widths at a depth of 1800 m

Pillar Width (m)	Maximum Tangential Stress with sequential excavation of tunnels (MPa)	Maximum Tangential Stress with simultaneous excavation of tunnels (MPa)
15	133.98	132.53
20	133.08	131.49
25	130.44	128.5
30	135.07	134.91
35	138.7	138.65
40	142.58	140.81
45	145.71	143.51
50	147.13	145.77
55	147.95	148.55
60	148.51	150.01
65	148.95	149.87
70	148.28	149.7

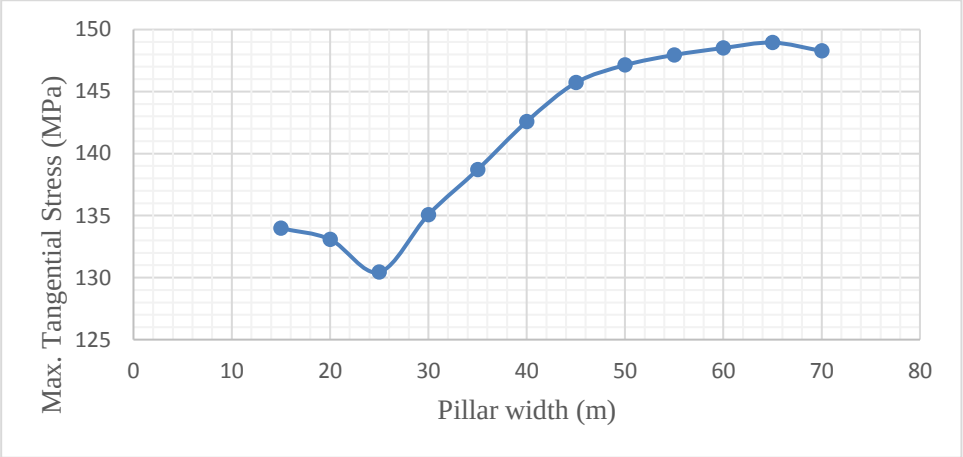

Figure 5.13: Relationship between max. tangential stress and pillar width at a depth of 1800 m for sequential excavation of tunnels

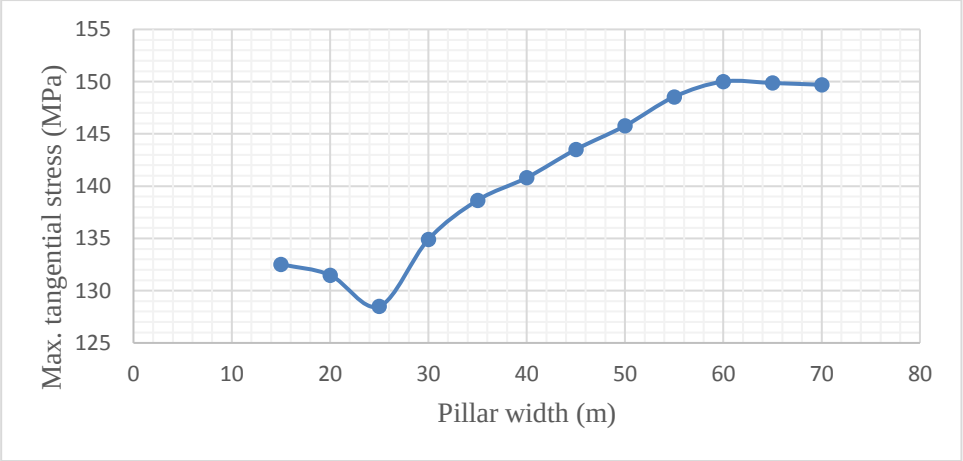

Figure 5.14: Relationship between max. tangential stress and pillar width at a depth of 1800 m for simultaneous excavation of tunnels

Figures 5.13 and 5.14 show that the maximum stresses experienced, in either case of separate or simultaneous excavation of tunnels, are at their lowest values for the pillar width of 25 m. So, a pillar width of 25 m is most suitable to keep the stresses at their minimum values.

5.3.4 Overburden Analysis (Linear Elastic Models)

As per proposed methodology, the rock burst assessment was also carried out considering the material to be elastic. In this section, tunnels are excavated in 2 stages. To predict the rock burst tendency, same procedure was adopted as discussed earlier in section 5.3.1. The assessment results for rock burst tendency, when excavating the tunnels separately, are presented in Tables 5.12 to 5.15.

Table 5.12: Rock burst assessment at the crown of Tunnel 1 at various depths

Depth (m)	σ_c (MPa)	σ_θ (MPa)	Distance of σ_θ from the crown (m)	Ts = σ_θ / σ_c	Rock burst tendency
200	86	24.43	0	0.28	No
500	86	61.61	0	0.72	Violent
800	86	98.79	0	1.15	Violent
1200	86	148.36	0	1.73	Violent
1500	86	185.14	0	2.15	Violent
1800	86	222.59	0	2.59	Violent

Table 5.13: Rock burst assessment at the invert of Tunnel 1 at various depths

Depth (m)	σ_c (MPa)	σ_θ (MPa)	Distance of σ_θ from the invert (m)	Ts = σ_θ / σ_c	Rock burst tendency
200	86	25.12	0	0.29	No
500	86	62.28	0	0.72	Violent
800	86	99.44	0	1.16	Violent
1200	86	148.98	0	1.73	Violent
1500	86	186.14	0	2.16	Violent
1800	86	223.12	0	2.59	Violent

Table 5.14: Rock burst assessment at the crown of Tunnel 2 at various depths

Depth (m)	σ_c (MPa)	σ_θ (MPa)	Distance of σ_θ from the crown (m)	Ts = σ_θ / σ_c	Rock burst tendency
200	86	23.16	0	0.27	No
500	86	58.41	0	0.68	Strong
800	86	93.67	0	1.09	Violent
1200	86	140.68	0	1.64	Violent
1500	86	175.94	0	2.05	Violent
1800	86	211.25	0	2.46	Violent

Table 5.15: Rock burst assessment at the invert of Tunnel 2 at various depths

Depth (m)	σ_c (MPa)	σ_θ (MPa)	Distance of σ_θ from the invert (m)	Ts = σ_θ / σ_c	Rock burst tendency
200	86	23.88	0	0.28	No
500	86	59.23	0	0.69	Strong
800	86	94.56	0	1.10	Violent
1200	86	141.66	0	1.65	Violent
1500	86	176.99	0	2.06	Violent
1800	86	211.45	0	2.46	Violent

From these tables, it can be observed that the tangential stress acting at the tunnel are much higher in linear elastic models as compared to elasto-plastic models. This comparison is shown in Table 5.16. Another observation that is significant here, is that the distance of concentration of stresses from the tunnel perimeter is zero that is the maximum stress is being applied at the periphery of the tunnel without their accumulation behind the tunnel periphery as was observed in elasto-plastic models. The tendency of rock burst is almost similar at the crown and the invert of the tunnels.

Table 5.16: Comparison of maximum tangential stresses with sequential excavation of tunnels in Linear Elastic and Elasto-Plastic models.

Depth (m)	Maximum Tangential Stress with sequential excavation of tunnels in Elasto-Plastic Models (MPa)	Maximum Tangential Stress with sequential excavation of tunnels in Linear Elastic Models (MPa)
200	23.77	25.12
500	43.88	62.28
800	69.69	99.44
1200	102.77	148.98
1500	113.11	186.14
1800	136.61	223.12

Figure 5.15 shows the comparison of maximum tangential stresses acting on tunnels in linear elastic and elasto-plastic models for sequential excavation of tunnels.

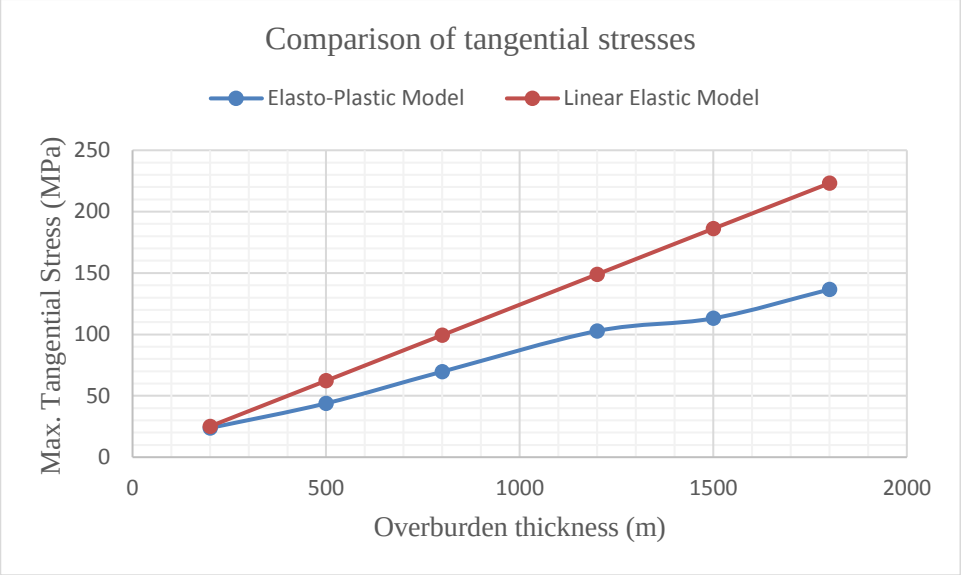

Figure 5.15: Comparison of tangential stresses in linear elastic and elasto-plastic models

It is clear from the Figure 5.15 that the linear elastic model is highly overestimating the stress values as the maximum stresses in linear elastic model are much higher than the elasto-plastic model.

5.3.5 Excavation sequence analysis (Linear Elastic Models)

To analyze the effect of excavation sequence in linear elastic models, stress redistribution and rock burst assessment was evaluated by excavating both tunnels simultaneously. The assessment results are given in Tables 5.17-5.20. A comparison of maximum tangential stresses acting in linear elastic and elasto-plastic models for simultaneous excavation of tunnels in presented in Table 5.21 and a comparison of maximum tangential stresses for sequential and simultaneous excavation of tunnels in linear elastic models in presented to analyze the effect of excavation sequence on rock burst occurrence.

Table 5.17: Rock burst assessment at the crown of Tunnel 1 at various depths

Depth (m)	**σ_c (MPa)**	**σ_θ (MPa)**	**Distance of σ_θ from the crown (m)**	**Ts = σ_θ / σ_c**	**Rock burst tendency**
200	86	23.11	0	0.27	No
500	86	58.31	0	0.68	Strong
800	86	93.46	0	1.09	Violent
1200	86	140.42	0	1.63	Violent
1500	86	175.62	0	2.04	Violent
1800	86	210.81	0	2.45	Violent

Table 5.18: Rock burst assessment at the invert of Tunnel 1 at various depths

Depth (m)	σ_c (MPa)	σ_θ (MPa)	Distance of σ_θ from the invert (m)	Ts = σ_θ / σ_c	Rock burst tendency
200	86	23.78	0	0.28	No
500	86	58.92	0	0.69	Strong
800	86	94.02	0	1.09	Violent
1200	86	140.93	0	1.64	Violent
1500	86	176.07	0	2.05	Violent
1800	86	211.22	0	2.46	Violent

Table 5.19: Rock burst assessment at the crown of Tunnel 2 at various depths

Depth (m)	σ_c (MPa)	σ_θ (MPa)	Distance of σ_θ from the crown (m)	Ts = σ_θ / σ_c	Rock burst tendency
200	86	23.16	0	0.27	No
500	86	58.41	0	0.68	Strong
800	86	93.69	0	1.09	Violent
1200	86	140.33	0	1.63	Violent
1500	86	175.94	0	2.05	Violent
1800	86	211.2	0	2.46	Violent

Table 5.20: Rock burst assessment at the invert of Tunnel 2 at various depths

Depth (m)	σ_c (MPa)	σ_θ (MPa)	Distance of σ_θ from the invert (m)	Ts = σ_θ / σ_c	Rock burst tendency
200	86	23.9	0	0.28	No
500	86	59.23	0	0.69	Strong
800	86	94.17	0	1.10	Violent
1200	86	141.66	0	1.65	Violent
1500	86	176.99	0	2.06	Violent
1800	86	212.31	0	2.47	Violent

Table 5.21: Comparison of maximum tangential stresses in linear elastic and elasto-plastic models for simultaneous excavation of tunnels

Depth (m)	Maximum Tangential Stress with simultaneous excavation of tunnels in Elasto-Plastic Models (MPa)	Maximum Tangential Stress with simultaneous excavation of tunnels in Linear Elastic Models (MPa)
200	22.89	23.90
500	42.56	59.23
800	67.73	94.17
1200	96.84	141.66
1500	110.01	176.99
1800	135.05	212.31

Table 5.22: Comparison of maximum tangential stresses for sequential and simultaneous excavation of tunnels in linear elastic models

Depth (m)	Maximum Tangential Stress with sequential excavation of tunnels (MPa)	Maximum Tangential Stress with simultaneous excavation of tunnels (MPa)
200	25.12	23.90
500	62.28	59.23
800	99.44	94.17
1200	148.98	141.66
1500	186.14	176.99
1800	223.12	212.31

The comparison given in Table 5.21 and Table 5.22 is also illustrated in Figure 5.16 and Figure 5.17, respectively to visualize the trend in values.

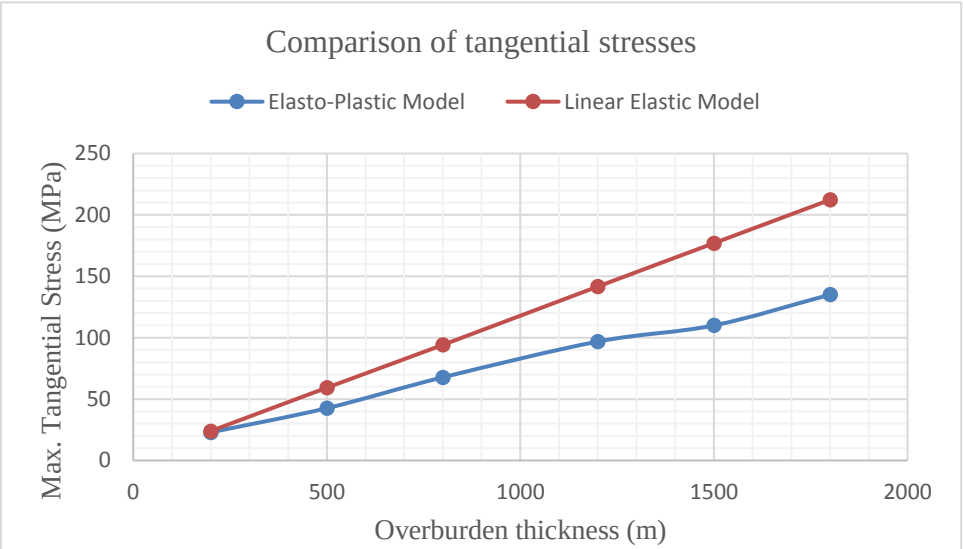

Figure 5.16: Comparison of tangential stresses in linear elastic and elasto-plastic models

Figure 5.16 shows reasonable high values of tangential stresses in linear elastic models as compared to elasto-plastic models thereby suggesting that the linear elastic models do not provide the true estimation of stresses as stated by Abdellah (2013). Therefore, elasto-plastic models are the best choice to have the approximate true picture of stress regime around underground openings. Figure 5.17 illustrates the effect of excavation sequence on stress redistribution and suggests that the maximum tangential stress acting on the parallel tunnels are slightly lower when both tunnels are excavated simultaneously as compared to sequential excavation of tunnels.

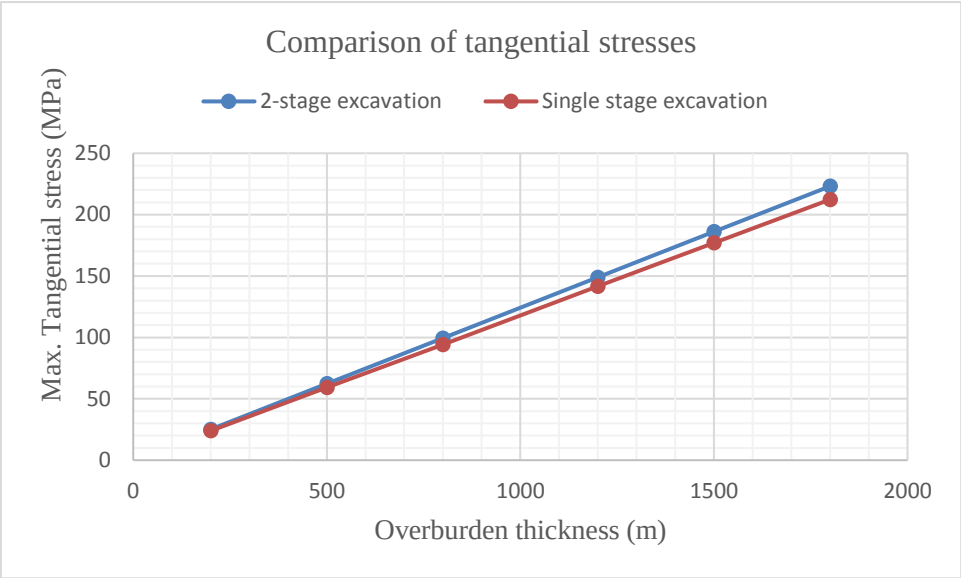

Figure 5.17: Comparison of tangential stresses for sequential and simultaneous excavation of tunnels

However, this decrease is not significant enough to have an impact on rock burst occurrence. Therefore, the excavation sequence doesn't have much effect in decreasing the possibilities of rock burst occurrence.

5.4 Support requirements of the tunnels

To analyze the support requirements of the tunnels, yielded elements and total displacements of the tunnels are analyzed for following conditions:

- No support
- Rock bolts
- Liners

Two types of rock bolts (End-anchored, Swellex) are installed with a length of 8 m (as suggested by Q-value) for different bolt spacing ranging from 0.5 m to 2 m. Effect of rock bolts on yielded elements and total displacement is shown in Figures 5.20 and 5.21.

Two types of reinforced concrete liners are installed. One of them was reinforced with wire mesh having a wire spacing of 0.2 m and the other was reinforced with I-beams with a beam spacing of 0.5 m. The effect of liners on the tunnels is shown in Figures 5.22 to 5.25.

5.4.1 Tunnels with no support

Figure 5.18 shows the yielded elements of the tunnels when unsupported. It shows the depth of yielded elements in the crown is 2.5 m and 3 m in the invert of the tunnels. However, the yielding in the sides of the tunnels is negligible.

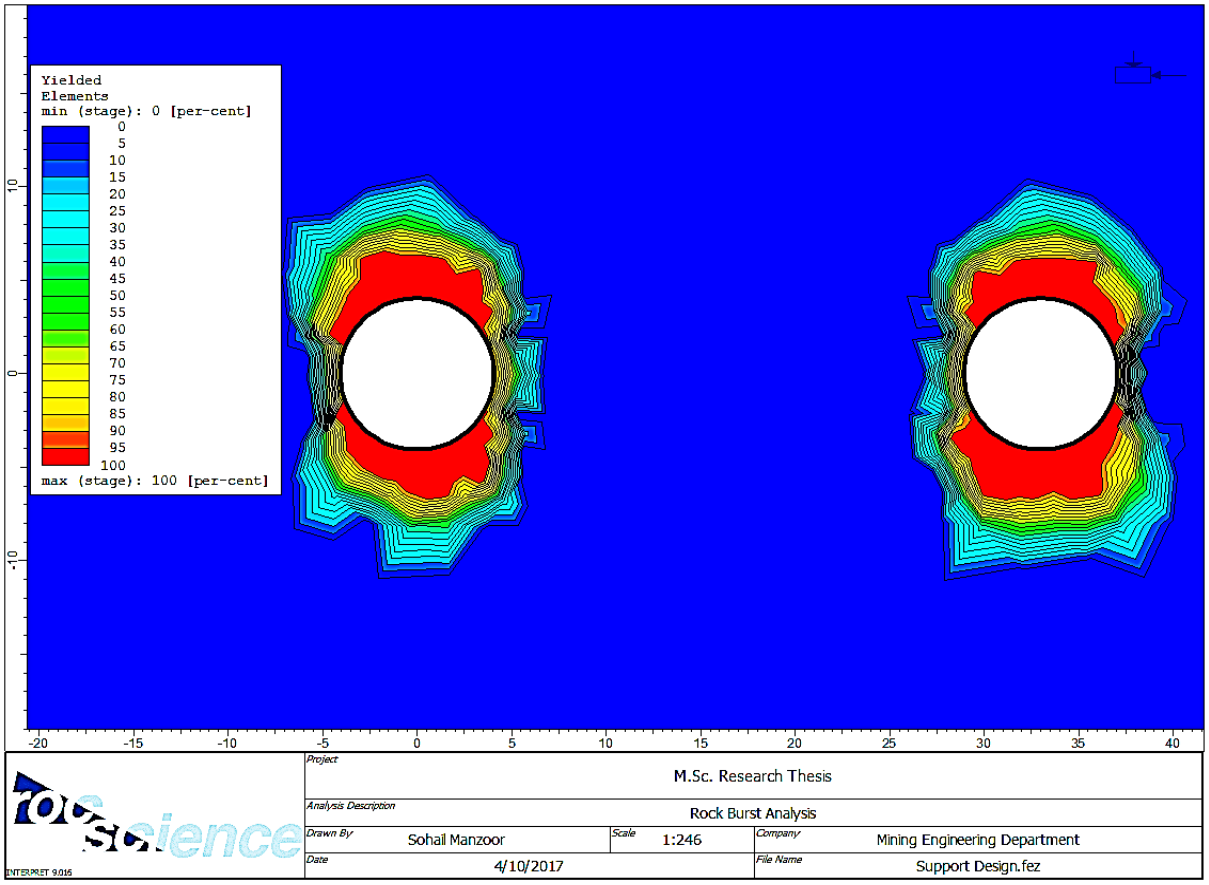

Figure 5.19: Yielded elements of tunnels under unsupported conditions

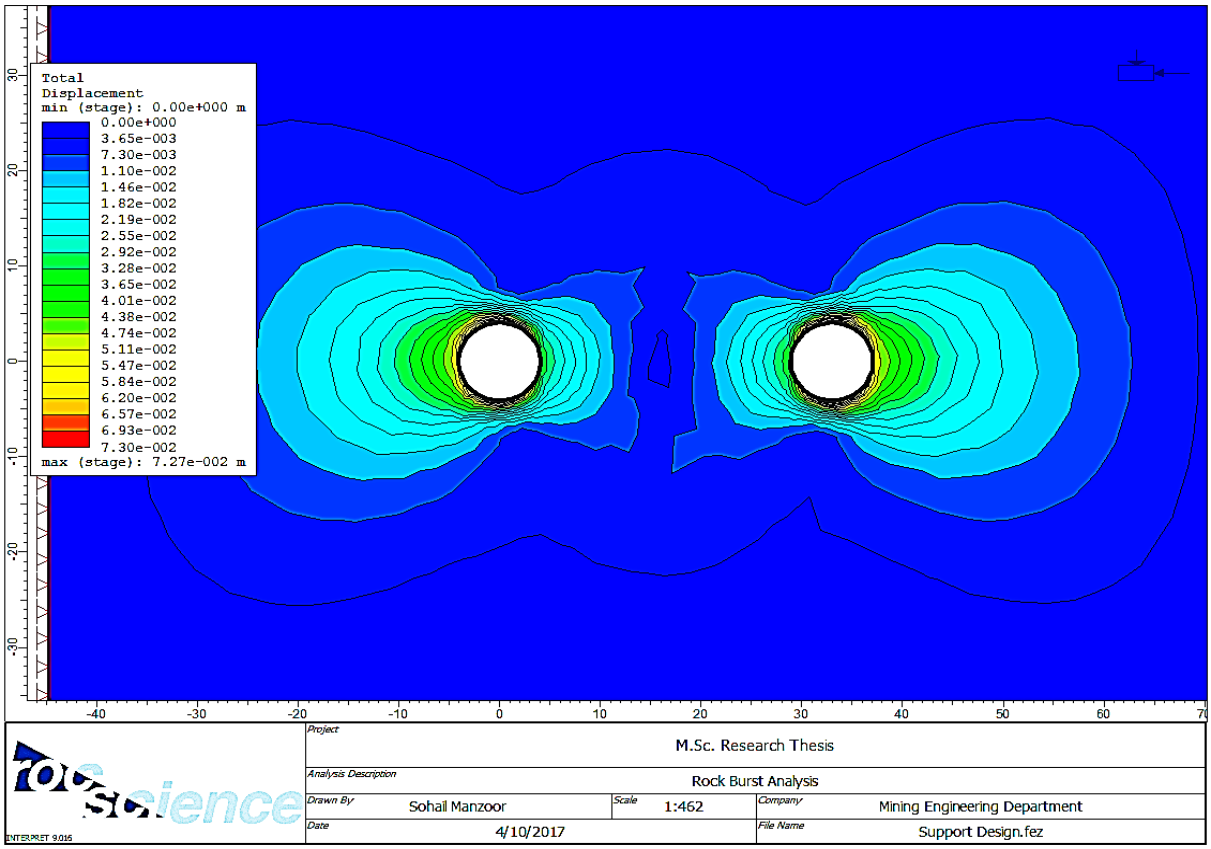

Figure 5.18: Total displacement of the tunnels under unsupported conditions

Figure 5.19 shows the total displacement of the tunnels under unsupported conditions. It shows the maximum total displacement of the tunnels is 17.76 m.

5.4.2 Tunnels with rock bolts

End-anchored and Swellex rock bolts are installed and their effect on yielded elements and total displacement of tunnels is observed. Analysis is carried out for varying bolt spacing. Results are shown in Figures 5.20 and 5.21.

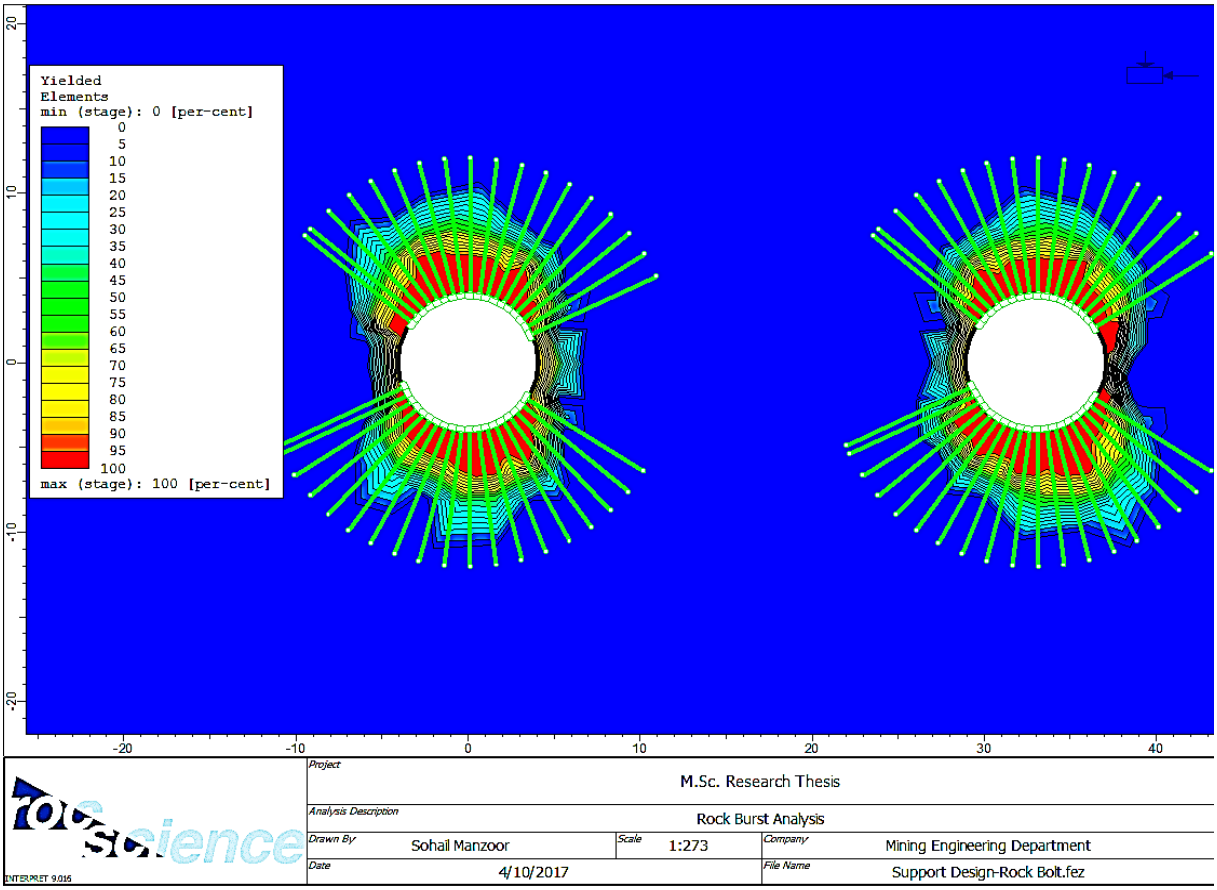

Figure 5.20: Yielded elements of the tunnels with installed rock bolts

Figure 6.20 shows that there is negligible effect of rock bolting on yielded elements. The depth of yielded elements is almost the same as it was for unsupported conditions. The effect was the similar for both types of rock bolts that is end-anchored and Swellex rock bolts with varying bolt spacing. Bolt installation did not affect the yielding of the tunnels considerably.

Figure 6.21 shows that there is slight decrease in total displacement of the tunnels that can be regarded as negligible. The maximum total displacement for this case is 17.41 m while it was 17.76 m for unsupported conditions. So, bolt installation did not affect the total displacement of the tunnel considerably as well.

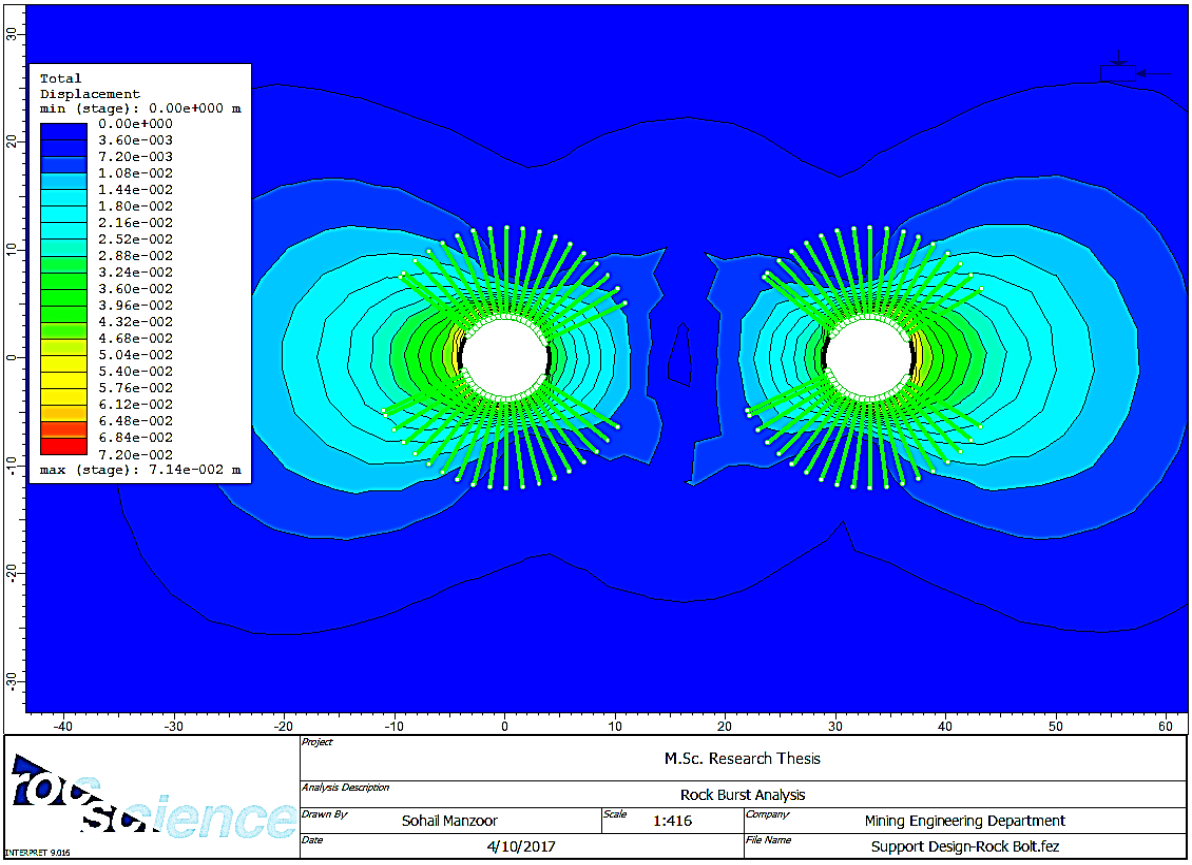

Figure 5.21: Total displacement of the tunnels with installed rock bolts

5.4.3 Tunnels with concrete liners

Reinforced concrete liners having reinforcement of wire mesh and I-beams are installed to analyze the effect of tunnel yielding and displacement. The effect of liners on tunnels is shown in Figures 5.22 to 5.25.

Figure 5.22 shows tunnels with wire mesh reinforced concrete liners and their effect on yielding of the tunnels. It is clear from the figure that the depth of the yielding elements is considerable decreased in the crown of the tunnel (1.5 m) and at the invert of the tunnel (1.0 m) as compared to unsupported conditions.

Figure 5.23 shows tunnels with wire mesh reinforced concrete liners and their effect on total displacement of the tunnels. It can be seen that the total displacement of the tunnels has reduced significantly from 17.76 m for unsupported conditions to 7.46 m for liner support. So, wire mesh reinforced concrete has better results than rock bolting in terms of yielding and total displacement of the tunnels.

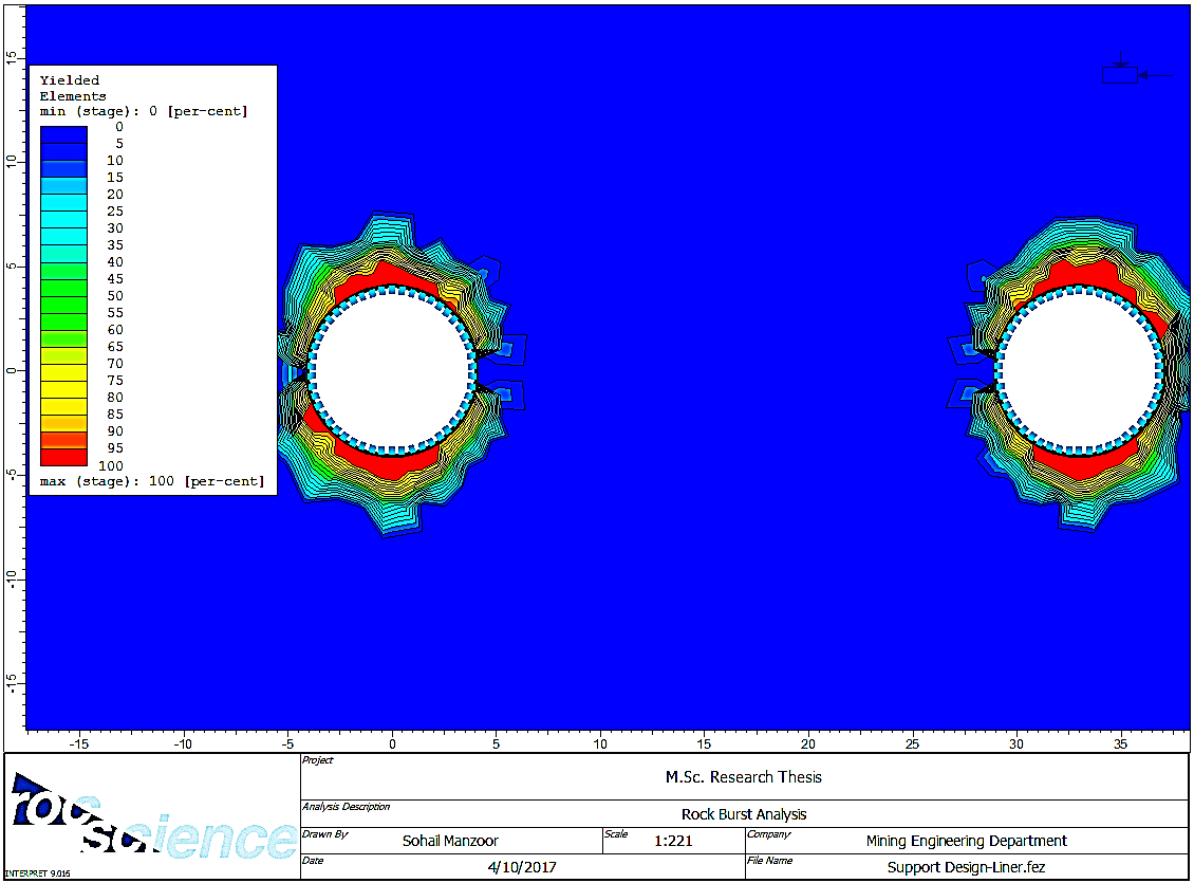

Figure 5.23: Total displacement of tunnels with wire mesh reinforced concrete liner

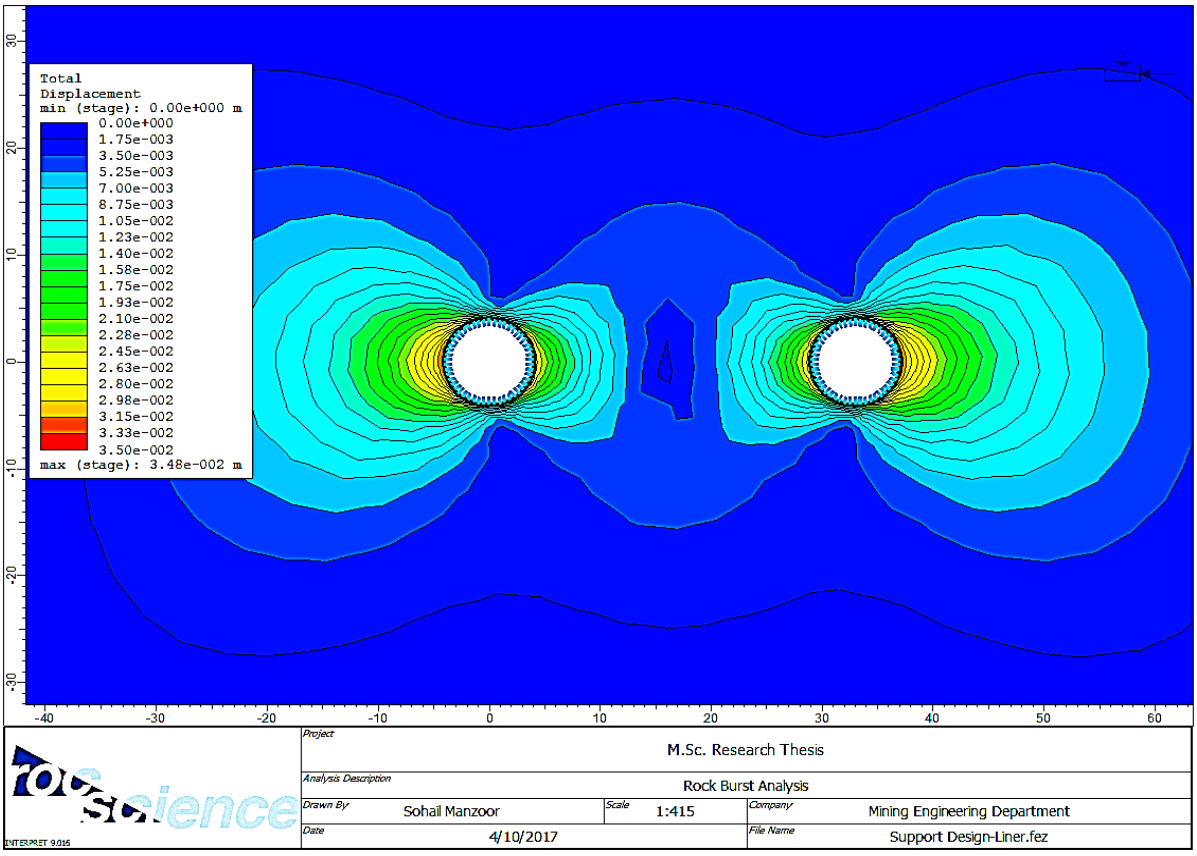

Figure 5.22: Yielded elements of the tunnels with wire mesh reinforced concrete liner

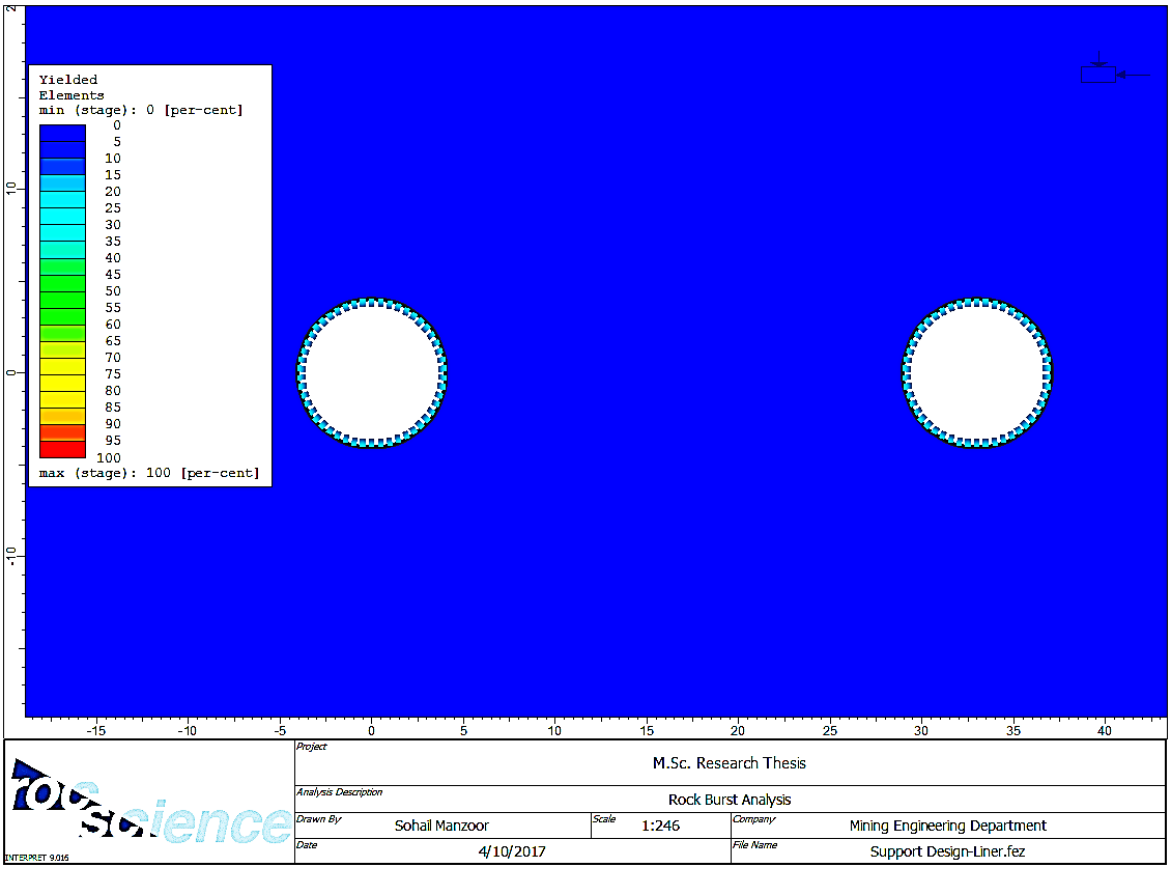

Figure 5.24: Total displacement of the tunnels with I-Beam reinforced concrete liner

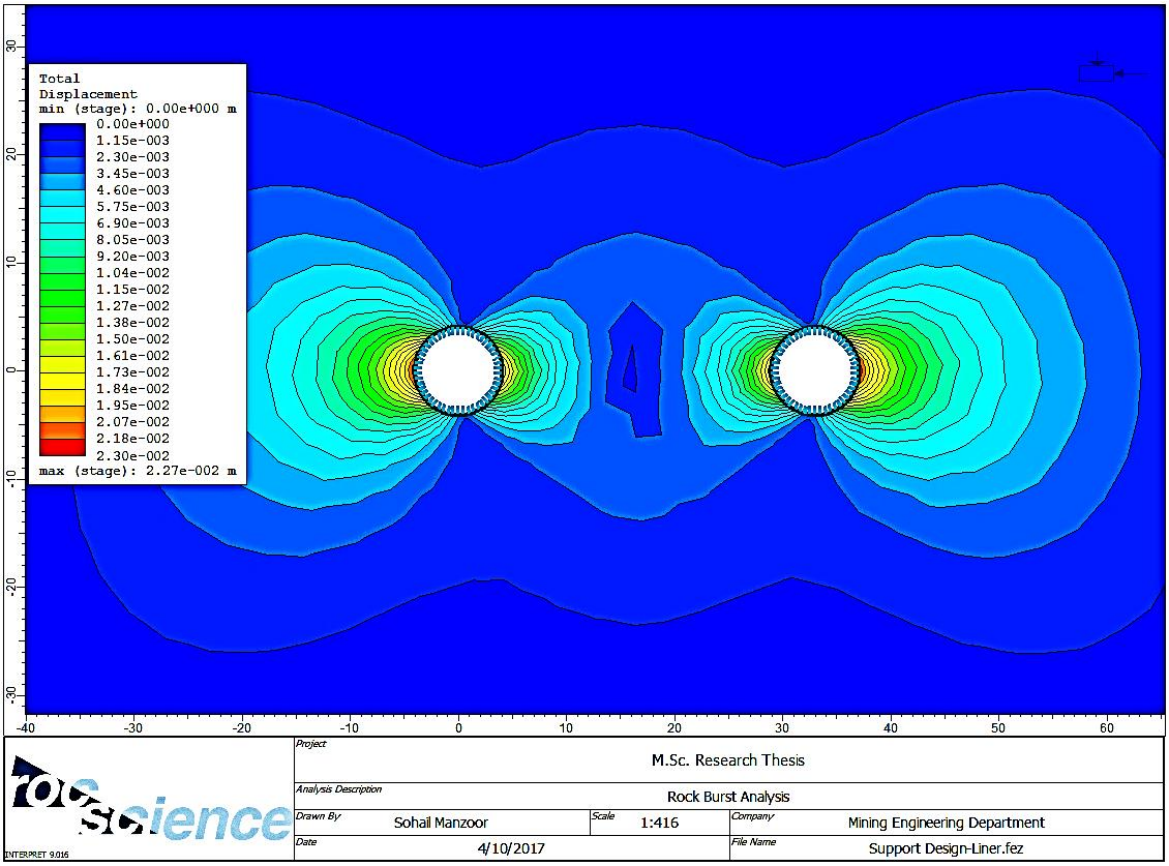

Figure 5.25: Yielded elements of the tunnels with I-Beam reinforced concrete liner

Figure 5.24 shows the effect of I-beam reinforced concrete liner on yielded elements of the tunnels. It is clear from the figure that the liner has eliminated the yielding phenomenon of the tunnel. There is no yielding of the tunnel at all. Figure 5.25 shows the reduction of total displacement after the installation of concrete liner. So, the I-beam reinforced concrete liner is the best choice to limit the yielding and displacement of the tunnels.

5.5 Elastic strain energy criterion

The stored elastic strain energy per unit volume of the rock is called the elastic strain energy density (SED). The elastic SED is an important factor to identify the potential for rockburst phenomenon in underground excavations (Sepehri, 2016).

For a rock specimen under the UCS test, using the principal of conservation of energy and the linear elasticity theory, the storage elastic SED can be calculated using equation (2.2).

$$\text{SED} = \frac{\sigma c^2}{2Es}$$

where σc is the UCS and Es is the Young's modulus in the unloading curve.

According to the study by (Sepehri, 2016), based on the value of the SED, the rockburst intensity in a rock mass can be classified into four groups. The result of this rating system is presented as under:

Investigation reveals that the occurrence of rock burst could be predicted and scaled by the so-called potential energy of elastic strain, PES, that is given by:

SED < 40 kJ/m3, then the rock burst hazard is low;
40 ≤ SED < 100 kJ/m3, then the rock burst hazard is moderate;
100 ≤ SED < 200 kJ/m3, then the rock burst hazard is strong;
SED ≥ 200 kJ/m3, then the rock burst hazard is very high.

The UCS of the rock mass in our potential project site is 86 MPa and Es is 11880 MPa. The SED for our project site is given as under:

$$\text{SED} = (86)^2/2(11880)$$

$$\text{SED} = 311 \text{ kJ/m}^3$$

The value of SED clearly shows that there is a very high rock burst hazard for this rock mass and verifies the results of tangential stress criterion.

5.6 Summary

The FE analysis model and the tangential stress criterion for rock burst prediction were used as the basis of a methodology, developed in this chapter, for predicting the rockburst tendency in parallel tunnels. Both conventional and numerical methods have been combined to estimate the rockburst potentials in a potential hydro-electric project site.

The advantages of the proposed methodology presented in this chapter are as follows:

- It accounts for both mining-induced stresses (which is the environmental factor) and the strength characteristics of the rock (which is the physical properties of the rock).
- The impact of the in-situ stress state, excavation depth and excavation sequence are also considered in this method (with help of the FE analysis model).
- Utilizing the proposed methodology, potentially hazardous areas can be identified. The methodology can also assist in the planning and design of underground openings such that the high stresses and energy release induced by mining can be minimized.

Chapter 6 CONCLUSION, RECOMMENDATIONS AND FUTURE WORK

6.1 Conclusion

Rock mass classification of the project, applied in chapter 3, showed that the rock mass quality is good with a Q value 14 of and RMR value of 70. The support requirements as per RMR value are given as under;

- Shotcrete: 50 mm in crown where required
- Rock bolts (20 mm diameter, fully grouted): Locally, bolts in crown 3m long, spaced 2.5 m with occasional wire mesh

The support requirement as per Q value is given as under;

- Spot bolting with a bolt length of 8 m

The FE analysis model and the tangential stress criterion for rock burst assessment were used as the basis of the methodology, applied in chapter 5, for predicting the rockburst tendency in two parallel tunnels. Both conventional and numerical methods have been combined to estimate the rockburst potentials in potential hydro-electric project site tunnels.

The optimum pillar width between the parallel tunnels was 25 m. The tunnels are safe up to a depth of 200 – 300 m in terms of rock burst hazard. Simultaneous excavation of the tunnels is better choice than sequential excavation of tunnels to have the benefit of mutual impact of tunnels. I-beam reinforced concrete liners are the best choice to limit yielding and displacement of the tunnels.

6.2 Recommendations

Depending upon the literature review and FE modelling results, following recommendations are made to avoid or minimize the rock burst tendency in parallel tunnels:

- Drill and blast method is more suitable in rock bursting conditions as it allows some of stress relaxation in the skin of excavated area as compared to TBM excavation.

- Destress blasting is an important technique utilized to minimize the rock burst hazard. The depth of maximum stresses can be easily computed through FE models and destressing can be accomplished more effectively.
- Simultaneous excavation of tunnels is more favorable as compared to sequential excavation of parallel tunnels in terms of maximum stresses.
- A pillar width of 25 m is most suitable to minimize the stresses around the tunnels.
- I-beam reinforced concrete liners with I-beam spacing of 0.5 m is most suitable to avoid yielding of the tunnels.

6.3 Future work

The FE model and methods developed in this study provided an engineering methodology to estimate mining-induced stress regimes which can be used for predicting rock bursting in tunnels and underground hard rock mines. However, there is still a need for continued investigations into the use of this methodology in an underground environment. The following recommendations could improve the method and add to the body of knowledge in this research area:

- The numerical model generated in this study assumed that the rock mass is continuous. By introducing discontinuities, faults and joint sets into the model, more accurate results can be obtained. Furthermore, the effect of these discontinuities on the stability and release of excess energy in an underground tunneling or mining environment should be examined.
- Including more realistic rock mass fracturing systems into the model requires proposing a new methodology based on hybrid methods (for instance, combining FE and discrete fracturing network (FEM/DFN) methods).

REFERENCES

Abdellah, W., 2013. *Geotechnical Risk Assessment of Mine Haulage Drifts during the Life of a Mine Plan.,* s.l.: Department of Mining and Materials Engineering, McGill University, Montreal, Quebec, Canada..

Armero, F. & Kim, J., 2012. Three dimensional finite elements with embedded strong discontinuities to model material failure in the infinitesimal range. *International Journal for Numerical Methods in Engineering,* Volume 91, pp. 1291-1330.

Aydan, Ö., Ulusay, R. & Tokashiki, N., 2014. A New Rock Mass Quality Rating System: Rock Mass Quality Rating (RMQR) and Its Application to the Estimation of Geomechanical Characteristics of Rock Masses. *Rock Mechanics and Rock Engineering,* 47(4), pp. 1255-176.

Balke, W. & Hedley, D. G., 2004. Rockbursts: Case studies from North American hard-rock mines.. *Society for Mining, Metallurgy and Exploration Inc.*.

Bardet, J. P., 1989. Finite element analysis of rockburst as surface instability. *Computers and Geotechnics*, Volume 8, pp. 177-193.

Barton , N. R., 2002. Some new Q-value correlations to assist in site characterization and tunnel design. *International Journal of Rock Mechanics and Mining Sciences,* 39(2), pp. 185-216.

Bawden, F. W., 2011. Ground Control Using Cable and Rock Bolting.. In: P. Darling, ed. *SME Mining Engineering Handbook.* Littleton: Society for Mining, Metallurgy and Exploration Inc., pp. 616-617.

Bieniawski, Z. T., 1989. *Engineering rock mass classifications: a complete manual for engineers and geologists in mining, civil, and petroleum engineering.,* New York, Wiley: s.n.

Bieniawski, Z. T., 1993. Classification of rock masses for engineering: The RMR system and future trends.. In: J. A. Hudson, ed. *Comprehensive Rock Engineering, Volume 3.* Oxford, New York,: Pergamon Press, pp. 553-573.

Binder, L., 1978. Rockbursts in New York. *Tunnels and Tunneling,* 10(8), pp. 15-17.

Blair, D. P., 1993. Blast vibration control in the presence of delay scatter and random fluctuations between blast holes.. *International Journal of Numerical and Analytical Methods in Geomechanics.,* 17(3).

Bobet, A. et al., 2009. Numerical Models in Discontinuous media: Review of advances for rock mechanics applications. *Journal of Geotechnical and Geoenvironmental Engineering,* p. 1547.

Brady, B. H. & Brown, E. T., 1993. *Rock Mechanics for underground mining.* London: Chapman and Hall.

Broch, E. & Sorheim, S., 1984. Experiences from the planning, construction and supporting of a road tunnel subjected to heavy rockbursting.. *Rock Mechanics and Rock Engineering*, Volume 17, pp. 15-35.

Broch, E. & Sorheim, S., 1984. Experiences from the planning, construction and supporting of a road tunnel subjected to heavy rockbursting.. *Rock Mechanics and Rock Engineering*, 17(1), pp. 15-35.

Brown, E. T., 1988. *Forecast and control of the rockburst.* Beijing: Department of Science and Technology, Ministry of Water Conservancy and Electric Power, Hydropower Headquarter of Chinese People's Armed Police Force.

Cao, A. Y. et al., 2008. Focal mechanism caused by fracture or burst of a coal pillar. *Journal of China University of Mining and Technology*, 18(2), pp. 153-158.

Chakraborti, D., Konietzky, H. & Walter, K., 2012. A Comparative Study of Different Approaches for Factor of Safety Calculations by Shear Strength Reduction Technique for Non-linear Hoek-Brown Failure Criterion. *Journal of Geotechnical and Geological Engineering*, Volume 30, pp. 925-934.

De Borst, R., Remmers, J. C., Needleman, A. & Abellan, M. A., 2004. Discrete vs smeared crack models for concrete fracture: bridging the gap. *International Journal for Numerical and Analytical Methods in Geomechanics*, Volume 28, pp. 583-607.

Deere, D. U. & Deere, D. W., 1988. *The rock quality designation (RQD), indexin practice.*. Philadelphia, ASTM.

Dong, L. J., Li, X. B. & Peng, K., 2013. Prediction of rockburst classification using Random Forest. *Transactions of Nonferrous Metals Society of China*, Volume 23, pp. 472-477.

Dujc, J., Bostjan, B. & Ibrahimegovic, A., 2013. Stress-hybrid quadrilateral finite element with embedded strong discontinuity for failure analysis of plane stress solids. *International Journal for Numerical Methods in Engineering*, Volume 94, pp. 1075-1098.

Duo, L. M., Lu, C. P., Mu, Z. I. & Gao, M. S., 2009. Prevention and forecasting of rock burst hazards in coal mines. *Mining Science and Technology*, 19(5), pp. 585-591.

Fries, T. P. & Belytschko, T., 2010. The generalized/extended finite element method: An overview of the method and its applications. *International Journal for Numerical Methods in Engineering*, Volume 84, pp. 253-304.

Gao, M. S., Dou, L. M. & Zhang, N., 2008. Simulation of the relationship between roadway dynamic destruction and hypocenter parameters.. *Journal of China University of Mining & Technology*, 18(1), pp. 93-97.

Godwin, W. H., 2017. Rock Mass Classification. *Encyclopedia of Engineering Geology*.

Grimstad, E. & Barton, N., 1993. *Updating the Q-system for NMT*. Oslo, Norwegian Concrete Association.

Gu, J. et al., 2014. Mechanism of ejective rockburst and model testing technology.. *Chinese Journal of Rock Mechanics and Engineering.,* 33(6), pp. 1081-1089.

Guo, R., Pan, C. L. & Yu, R. C., 2003. *Theory and Technique of Mining Dealing with Hard Rock Deposits Liable to Rockburst,* Beijing: Metallurgical Industry Press.

Herbst, M. & Konietzky, H., 2012. Numerical modelling of natural rock formations toestimate stability using the example of a sandstonemassif in Saxony.. *Geomechanics and Tunneling,* 5(4), pp. 379-388.

Hoek, E., 1994. Strength of rock and rock masses. *International Society of Rock Mechanics News Journal,* 2(2), pp. 4-16.

Hoek, E., 2007. *Practical rock engineering.* s.l.:RocScience.

Hoek, E., Carranza-Torres, C. & Corkum, C., 2002. *Hoek-Brown failure criterion: 2002 edition.*. Toronto, s.n., pp. 267-273.

Hu, H. et al., 2011. Active velocity tomography for assessing rockburst hazards in a kilometer deep mine. *Mining Science and Technology (China),* Volume 21, pp. 673-676.

Ibrahimbegovic, A., 2009. *Nonlinear Solid Mechanics: Theoretical Formulations and Finite Element Solution Methods.* 1st ed. London: Springer.

Islam, M. R. & Faruque, M. O., 2012. Numerical modelling of slope stability consideration of an open-pit coal mine in the Phulbari Coal Basin, NW Bangladesh. *Electronic Journal of Geotechnical Engineering,* Volume 17, pp. 3717-3729.

Jarufe, J. A. & Vasquez, P., 2014. Numerical modelling of rock-burst loading for use in rock support design at Codelco's New Mine Level Project. *Mining Technology*, 123(3), pp. 120-127.

Jiang, Q., Feng, X., Xiang, T. & Su, G., 2010. Rockburst characteristics and numerical simulation based on a new energy index: a case study of a tunnel at 1500 m depth.. *Engineering Geology and Environment,* 69(3), pp. 353-363.

Jing, L., 2003. A reviewof techniques, advances and outstanding issues in numerical modelling for rock mechanics and rock engineering. *International Journal of Rock Mechanics & Mining Sciences,* Volume 40, p. 283–353.

Jing, L. & Hudson, J. A., 2002. Numerical methods in rock mechanics. *International Journal of Rock Mechanics & Mining Sciences,* Volume 39, p. 409–427.

Jin-shan, S., Qi-hu, Z. & Wen-bo, L., 2007. Numerical simulation of rock burst in circular tunnels under unloading conditions. *Journal of China University of Mining & Technology,* 17(4), pp. 552-556.

Kabwe, E. & Wang, Y., 2015. Review on rockburst theory and types of rock support in rockburst prone mines.. *Open Journal of Safety Science and Technology.,* December, Volume 5, pp. 104-121.

Kaiser, P. K. & Cai, M., 2012. Design of rock support system under rockburst condition.. *Journal of Rock Mechanics and Geotechnical Engineering,* Volume 4, pp. 215-227.

Kaiser, P. K., Tannant, D. D. & McCreath, D. R., 1996. *Canadian rockburst support handbook.* Sudbury: Geomechanics Research Centre.

Khanlari, G. R. & Ghaderi-Meybodi, R., 2011. *Analysis of rock burst in critical section of second part of Karaj-Tehran water supply tunnel.*. Munich, s.n., pp. 661-667.

Liang, Z. et al., 2013. Microseismic monitoring and numerical simulation of rock slope failure. *International Journal of Distributed Sensor Networks,* Volume 2013, p. 10.

Li, G., Liang, Z. Z. & Tang, C. A., 2014. Morphologic interpretation of rock failure mechanisms under uniaxial compression based on 3D multiscale high-resolution numerical modeling.. *Journal of Rock Mechanics and Rock Engineering.*.

Li, G. & Tang, C. A., 2015. A statistical meso-damage mechanical method for modeling trans-scale progressive failure process of rock.. *International Journal of Rock Mechanics and Mining Sciences,* Volume 74, p. 133–150.

Liu, L. et al., 2011. Tempo-spatial characteristics and influential factors of rockburst: a case study of transportation and drainage tunnels in Jinping II hydropower station. *Journal of Rock Mechanics and Geotechnical Engineering,* 3(2), pp. 179-185.

Lu, A. H., Mao, X. B. & Liu, H. S., 2008. Physical simulation of rock burst induced by stress waves.. *Journal of China University of Mining & Technology,* 18(3), pp. 401-405.

Malek, F., Sourineni, F. T. & Vasak, P., 2009. *Geomechhanics strategies for rockburst management at Vale Inco Vreighton Mine.* Toronto, s.n.

Malmgren, L., 2005. *Interaction between shotcrete and rock: Experimental and Numerical study.,* Lulea: Lulea University of Technology.

Mansurov, V. A., 2001. Prediction of rock bursts by analysis of induced seismicity data. *International Journal of Roch Mechanics and Mining Sciences,* 38(4), pp. 893-901.

Marinos, P., Hoek, E. & Marinos, V., 2006. Variability of the engineering properties of rock masses quantified by the geological strength index: the case of ophiolites with special emphasis on tunneling. *Bulleting of Engineering Geology and Environment,* 65(2), pp. 129-142.

Martin, C. D., 1997. Seventeenth Canadian Geotechnical Colloquium: The effect of cohesion loss and stress path on brittle rock strength.. *Canadian Geotechical Journal,* 34(5), pp. 698-725.

Martin, C. D. & Chandler, N. A., 1994. The progressive fracture of Lac du Bonnet granite.. *International Journal of Rock Mechanics, Mining Science & Geomechanics Abstracts,* 31(6), pp. 643-659.

Martin, C. D., Kaiser, P. K. & McCreath, D. R., 1999. Hoek-Brown parameters for predicting the depth of brittle failure around tunnels.. *Canadian Geotechnical Journal,* Volume 36, pp. 136-151.

Mitri, H. S., Tang, B. & Simon, R., 1999. FE modelling of mining-induced energy release and storage rates. *The Journal of The South African Institute of Mining and Metallurgy,* March/April.pp. 103-110.

Myrvang, A. & Grimstad, E., 1983. Rockburst problems in Norwegian Highway tunnels-recent case histories in rockbursts-Prediction and Control. *London: Insitute of Mines and Metallurgy,* pp. 133-139.

Nikolic, M., Ibrahimbegovic, A. & Miscevic, P., 2015. Brittle and ductile failure of rocks: embedded discontinuity approach for representing mode I and mode II failure mechanisms. *International Journal for Numerical Methods in Engineering.*

Nikolić, M., Roje-Bonacci, T. & Ibrahimbegović, A., 2016. Overview of the numerical methods for the modelling of rock mechanics problems. *Technical Gazette,* 23(2), pp. 627-637.

Ortlepp, W. D., 1979. *The Mechanism of a Rockburst.*. Nevada, ISRM, pp. 478-483.

Ortlepp, W. D., 1992. *The design of support for the containment of rockburst damage in tunnels-an engineering approach.*. Sudbury, ISRM, pp. 593-609.

Ortlepp, W. D. & Stacey, T. R., 1994. Rockburst Mechanisms in Tunnels and Shafts. *Tunneling and Underground Space Technology,* 01 November, 09(01), pp. 59-65.

Palmstorm, A., 1995. *Characterizing rockburst and squeezing by the rock mass index.* New Dehli, s.n.

Palmstorm, A., 1995. RMi - A system for characterizing rock mass strength for use in rock engineering. *Journal of rock mechanics and tunnelling technology,* 1(2), pp. 69-108.

Palmstorm, A. & Broch, E., 2006. Use and misuse of rock mass classification systems with particular reference to the Q-system.. *Tunnelling and Underground Space Technology,* 21(6), p. 575–593.

Panthi, K. K., 2011. *Assessment on stress induced instability in a tunnel project of the Himalaya.*. Beijing, s.n., pp. 1777-1782.

Panthi, K. K., 2012. Evaluation of rock bursting phenomena in a tunnel in the Himalayas.. *Bulletin of Engineering Geology and the Environment.,* November, Volume 71, pp. 761-769.

Per John, L., 1983. *Hard rock pillar strength estimation: An applied Emiprical Approach.*, Vancouvar: The University of British Columbia.

Prochazka, P. P., 2004. Application of discrete element methods to fracture mechanics of rockbursts.. *Engineering Fracture Mechanics,* Volume 71, pp. 601-618.

Rocscience Inc., 2016-2017. *RS2 (Rock and Soil 2-dimensional analysis program).* s.l.

Rocscience Inc., 2016. *RS2 Finite Element Analysis for Excavations and Slopes Software Version 9.0,* Toronto: s.n.

Saksala, T., Brancherie, D., Harari, I. & Ibrahimbegovic, A., 2015. Combined continuum damage-embedded discontinuity model for explicit dynamic fracture analyses of quasi-brittle materials. *International Journal for Numerical Methods in Engineering,* Volume 101, pp. 230-250.

Semadeni, T., 1991. *Rockburing in the Strathcona-Craig Haulage Drift. Internal Report.*, Canada: Falconbridge Ltd..

Sepehri, M., 2016. *Finite Element Analysis Model for Determination of In-situ and Mining Induced Stresses as a Function of Two Different Mining Methods Used at Diavik Diamond Mine,* Alberta: University of Alberta.

Shan, Z. G. & Yan, P., 2010. Management of rock bursts during excavation of the deep tunnels in Jinping II Hydropower Station. *Bulletin of Engineering Geology and the Environment,* 01 April, Volume 69, pp. 353-363.

Sharan, S. K., 1989. Finite element analysis of underground openings.. *International Journal for Numerical and Analytical Methods in Geomechanics,* Volume 13, pp. 565-570.

Sharan, S. K., 1992. Elastostatic analysis of infinite solids using fininte elements.. *International Journal for Numerical Methods in Engineering,* Volume 35, pp. 109-120.

Sharan, S. K., 1993. Elasto-plastic finite element analysis of underground openings using elastic supports.. *International Journal of Rock Mechanics and Mining Sciences & Geomechanics Abstracts,* 30(7), pp. 1291-1294.

Sharan, S. K., 2000. Elasto-plastic finite element analysis of a crack in an infinite plate.. *International Journal of Fracture,* 103(2), pp. 163-176.

Sharan, S. K., 2003. Elastic-brittle-plastic analysis of circular openings in Hoek-Brown media.. *International Journal of Rock Mechanics and Mining Sciences,* Volume 40, pp. 817-824.

Sharan, S. K., 2007. A fininte element perturbation method for the prediction of rockburst. *Computers and Structures,* Volume 85, pp. 1304-1309.

Shiyong, W., Feng, X. & Sousa, L. R., 2010. *Jinping II mega hydropower project, China.* s.l., A New Cycle, Porto., pp. 223-231.

Singh, B. & Geol, R. K., 1999. *Rock Mass Classification. A Practical Approach in Civil Engineering.* 1st ed. Amsterdam: Elsevier Science.

Sousa, R. L., 2010. *Risk analysis for tunneling projects.,* Cambridge: MIT.

Sperry, P. E. & Heuer, R. E., 1972. *Excavation and support of the Navajo Tunnel No. 3.*. New York, SME of AIME, pp. 539-571.

Stacey, T. R., 1989. *Boring in massive rocks - rock fracture problems.* Yeoville, South Africa, SANCOT, pp. 87-90.

Stacey, T. R. & Harte, N., 1989. *Deep level raise boring - prediction of rock problems.*. Rotterdam, A.A.Balkema, pp. 583-588.

Stacey, T. R. & Thompson, P. W., 1991. *A large borehole breakout.*. Rotterdam, A.A. Balkema, pp. 1019-1021.

Sweby, G. J., Dight, P. M. & Potvin, Y., 2014. *The use of numerical models for Ground Support Systems Optimisation: Applications, Methods and Challenges.* Yancouver, Canada, s.n.

Tang, C., 2010. Preliminary engineering application of microseismic monitoring technique to rockburst prediction in tunneling of Jinping II project. *Journal of Rock Mechanics and Geotechnical Engineering,* 2(3), pp. 193-208.

Tan, Y. A., 1989. The mechanism research of rockburst. *Hydrogeology & Engineering Geology,* Volume 1, pp. 34-38.

Viladkar, M. N., Noorzaei, J. & Godbole, P. N., 1994. Behaviour of infinite elements in an elasto-plastic domain.. *Computers and Structures,* 51(4), pp. 337-342.

Wang, J. A. & Park, H. D., 2001. Comprehensive prediction of rockburst based on analysis of strain energy in rocks. *Tunnelling and Underground Space Technology,* Volume 16, pp. 29-57.

Wen, Z. et al., 2016. A study of rockburst hazard evaluation method in coal mine. *Shock and Vibration,* p. 9.

Woldemedhin, Y. B. & Mwagalanyi, H., 2011. *Investigation of rock fall and support damage induced by seismic motion at Kiirunavaara Mine,* Lulea: Lulea University.

Yi, C. P. et al., 2016. *Numerical modelling of dynamic response of underground openings under blasting based on field tests.* Luleå, s.n.

Yu, Q. et al., 2015. Study on rockburst nucleation process of deep-buried tunnels based on microseismic monitoring. *Shock and Vibration,* Volume 2015, p. 17.

Zhang, X. C. & Wang, J. Q., 2007. Research on the mechanism and prevention of rockburst at the Yinxin Gold Mine. *Journal of China University of Mining and Technology,* 17(4), pp. 541-545.

Zienkiewicz, O. C. & Taylor, R. L., 1989. *The finite element method, 4th Ed.*. London: McGraw-Hill.